

**Nato Advanced Research Workshop
Metallic Materials with High Structural Efficiency**

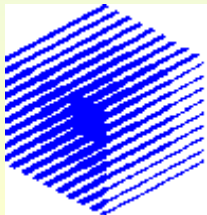
Kiev September 7th – 13th 2003

**Neutron and synchrotron
non-destructive methods for the
characterisation of materials
for different applications**

Franco Rustichelli



*Department of Sciences Applied to Complex Systems,
Polytechnic University of Marche – Ancona (Italy)*



*INFN - Istituto Nazionale per la Fisica della Materia Research
Unit of Ancona*

Report Documentation Page

Form Approved
OMB No. 0704-0188

Public reporting burden for the collection of information is estimated to average 1 hour per response, including the time for reviewing instructions, searching existing data sources, gathering and maintaining the data needed, and completing and reviewing the collection of information. Send comments regarding this burden estimate or any other aspect of this collection of information, including suggestions for reducing this burden, to Washington Headquarters Services, Directorate for Information Operations and Reports, 1215 Jefferson Davis Highway, Suite 1204, Arlington VA 22202-4302. Respondents should be aware that notwithstanding any other provision of law, no person shall be subject to a penalty for failing to comply with a collection of information if it does not display a currently valid OMB control number.

1. REPORT DATE 18 MAR 2004		2. REPORT TYPE N/A		3. DATES COVERED -	
4. TITLE AND SUBTITLE Neutron and synchrotron non-destructive methods for the characterisation of materials for different applications				5a. CONTRACT NUMBER	
				5b. GRANT NUMBER	
				5c. PROGRAM ELEMENT NUMBER	
6. AUTHOR(S)				5d. PROJECT NUMBER	
				5e. TASK NUMBER	
				5f. WORK UNIT NUMBER	
7. PERFORMING ORGANIZATION NAME(S) AND ADDRESS(ES) Department of Sciences Applied to Complex Systems, Polytechnic University of Marche Ancona (Italy)				8. PERFORMING ORGANIZATION REPORT NUMBER	
9. SPONSORING/MONITORING AGENCY NAME(S) AND ADDRESS(ES)				10. SPONSOR/MONITOR'S ACRONYM(S)	
				11. SPONSOR/MONITOR'S REPORT NUMBER(S)	
12. DISTRIBUTION/AVAILABILITY STATEMENT Approved for public release, distribution unlimited					
13. SUPPLEMENTARY NOTES See also ADM001672., The original document contains color images.					
14. ABSTRACT					
15. SUBJECT TERMS					
16. SECURITY CLASSIFICATION OF:			17. LIMITATION OF ABSTRACT	18. NUMBER OF PAGES	19a. NAME OF RESPONSIBLE PERSON
a. REPORT	b. ABSTRACT	c. THIS PAGE			
NATO/unclassified	unclassified	unclassified	UU	55	

MMCs mechanical properties

TOUGHNESS

HARDNESS

DUCTILITY

MMCs replace
steel and cast iron
in automotive components

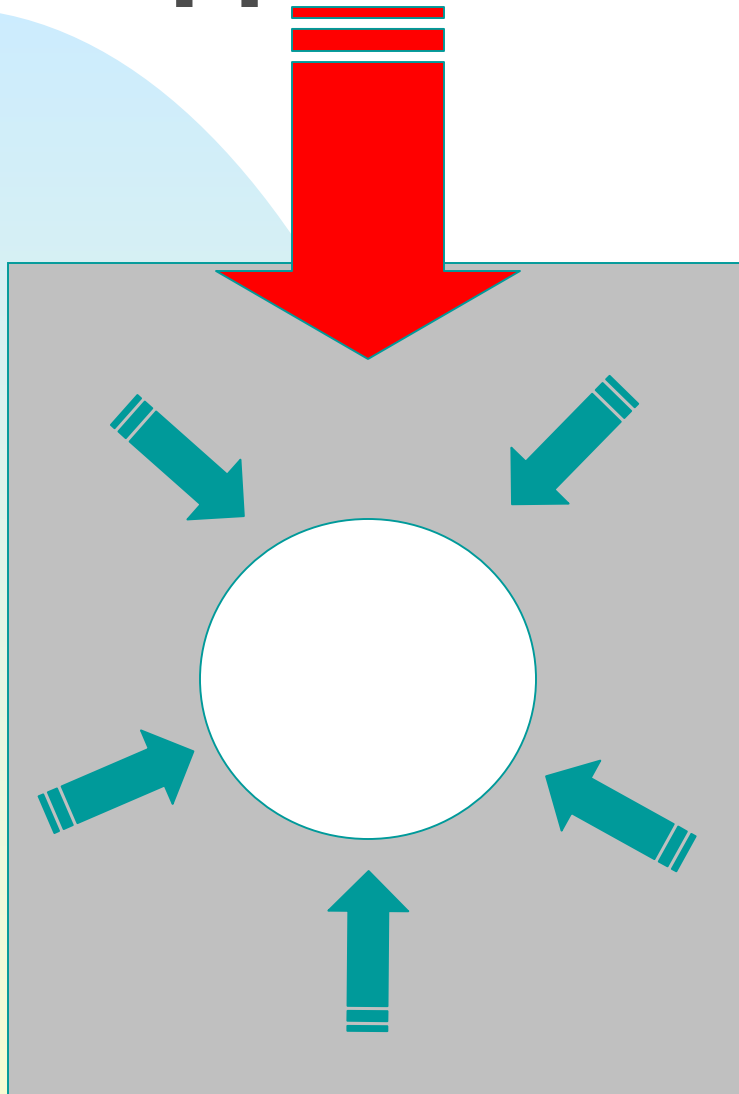
LIGHT WEIGHT

STRENGTH

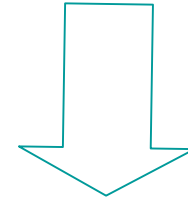
Metal Matrix

**Ceramic
Reinforcement**

Applied load



Load transfer



$$(1 - f) \langle \sigma_M \rangle + f \langle \sigma_I \rangle = \sigma_A$$

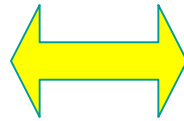
- Volume fraction (f);
- Reinforcement shape;
- Reinforcement orientation;
- Elastic properties of both phases.

Large reinforcement size

High applied/residual
stress

Particle clustering

Nucleation of precipitates



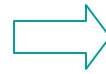
Formation of voids

Crack initiation

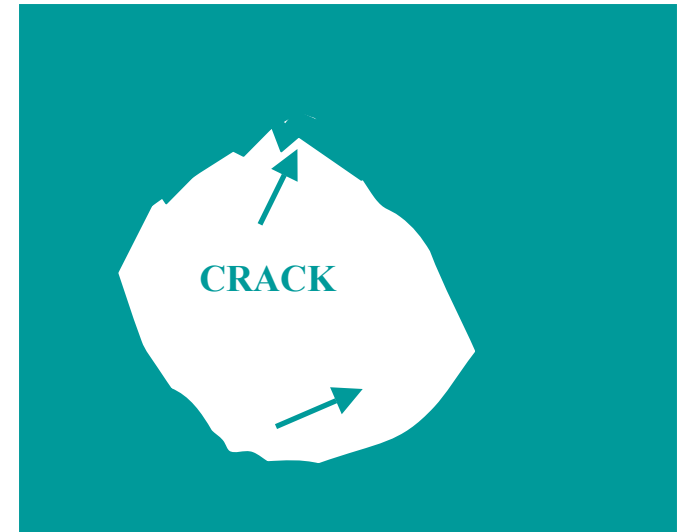
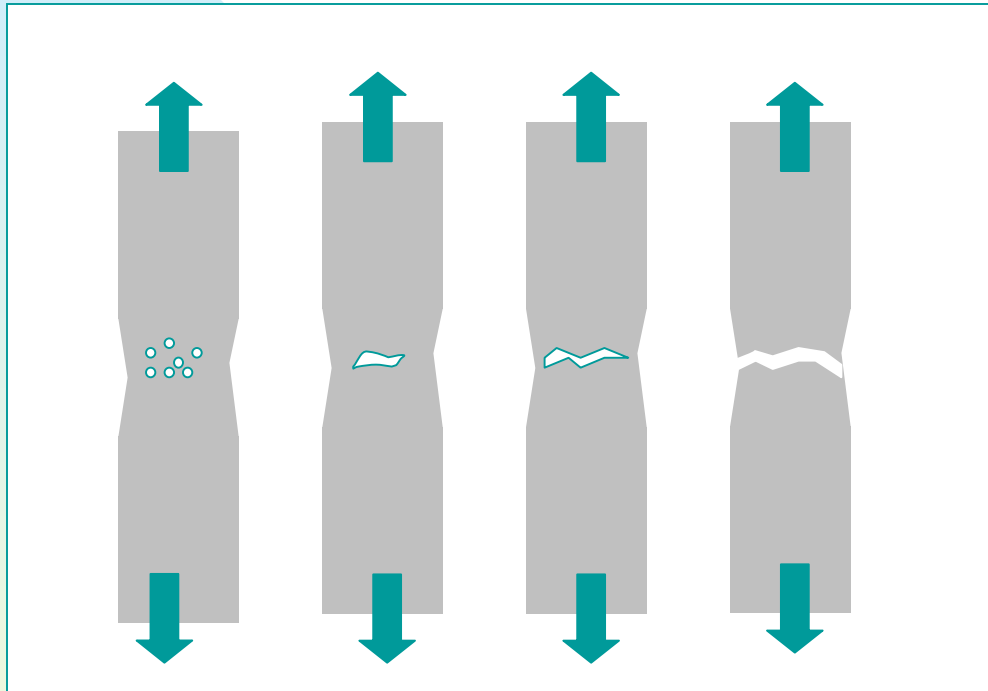
Fracture

Ductile fracture:

- after high plastic deformation

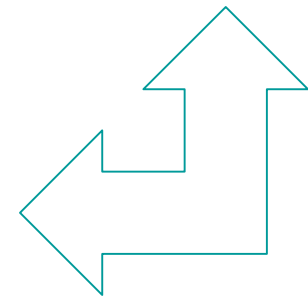


Excess of internal stress



Internal Stress Analysis

before/after thermal/mechanical treatments



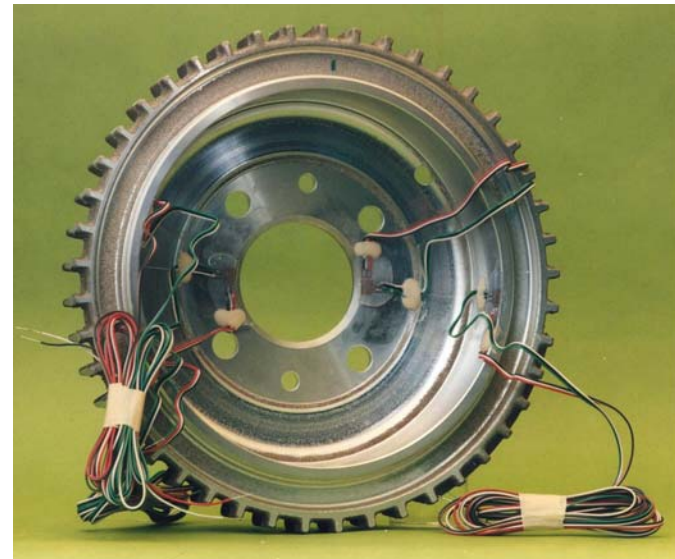
Brake Drum (AA359 + 20 vol. % SiCp)

3 identical brake drums → Die-casting → T6 heat treatment

Disamatic low pressure sand
mould casting

Solubilization: 560°C x 2 hours;
Quenching: H₂O at 20°C;
Aging: 177°C x 10 hours.

- 1) as-cast brake drum
- 2) 15000 N for 2065000 cycles
25000 N for 2600000 cycles
30000 N for 2500000 cycles
35000 N for 2500000 cycles
- 3) broken after 782000
cycles at 25000 N



MMC Residual Stress Calculation:

$$\sigma_{tot}^i = \sigma_{macro} + \sigma_{mE}^i + \sigma_{mT}^i$$

$i = \text{Matrix, Reinforcement}$

Difference in elastic constants of the two phases

Difference in thermal expansion coefficients of the two phases

$$\sigma_{macro} = f \sigma_{tot}^{reinf.} + (1 - f) \sigma_{tot}^{matrix}$$

$f = \text{volume fraction of the reinforcement phase}$

$$\sigma_{mE}^i = \mathbf{B}^i \sigma_{macro}$$

$\mathbf{B}^i = \text{tensor depending on reinforcement shape and elastic constants of the reinforcement and the matrix. Calculated on the basis of Eshelby's "equivalent homogeneous inclusion" model.}$

➤ Before bench test

- Instrument: Neutron Diffractometer G5.2, LLB of Saclay (F)
- Wavelength: 0.316 nm
- Gauge Volume: 2x2x2 mm³
- Diffracting plans: (200) for Al, (311) for SiC

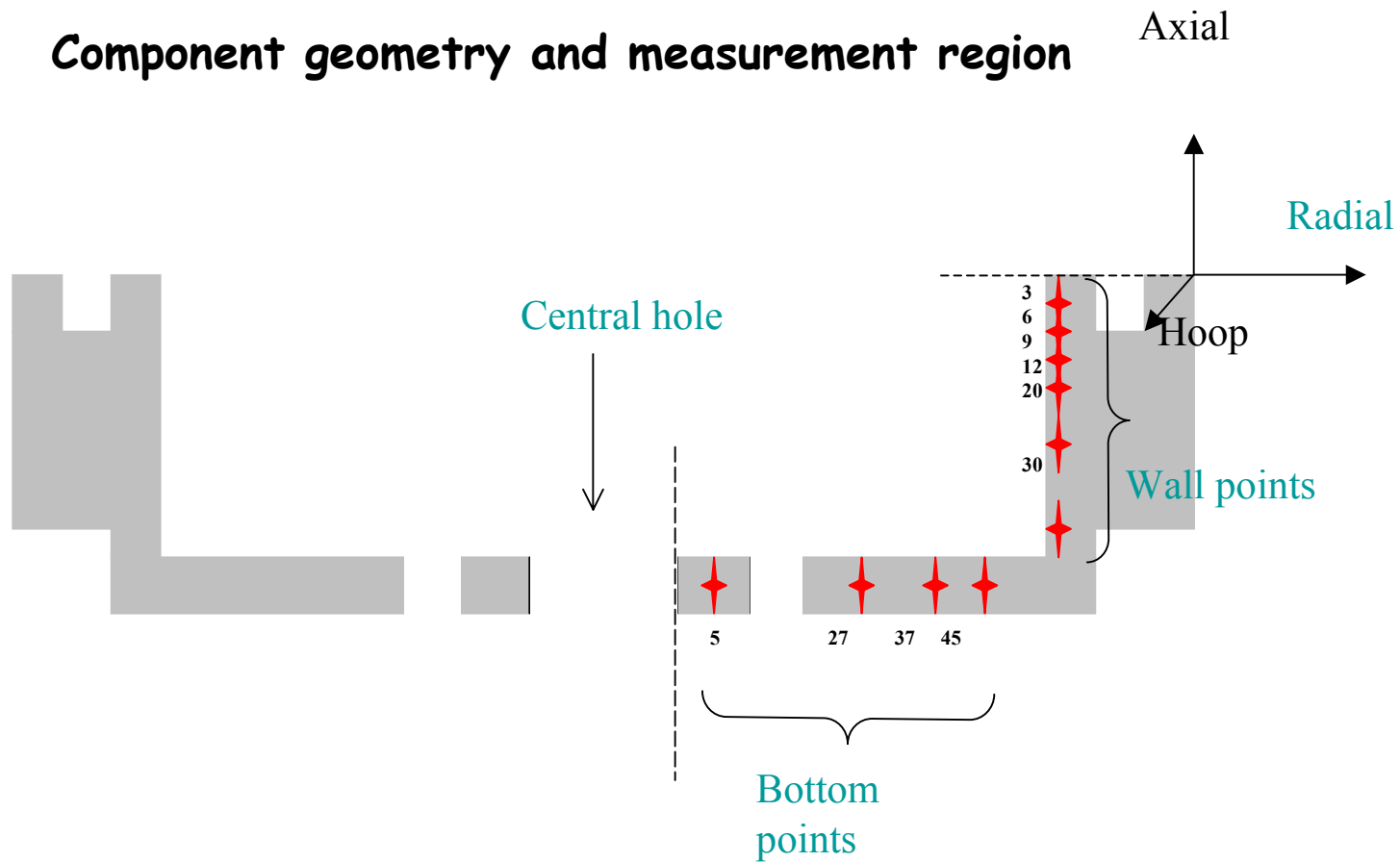
After bench test without breaking

- Instrument: Neutron Diffractometer G5.2, LLB of Saclay (F)
- Wavelength: 0.316 nm
- Gauge Volume: 2x2x2 mm³
- Diffracting plans: (200) for Al, (311) for SiC

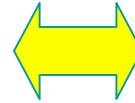
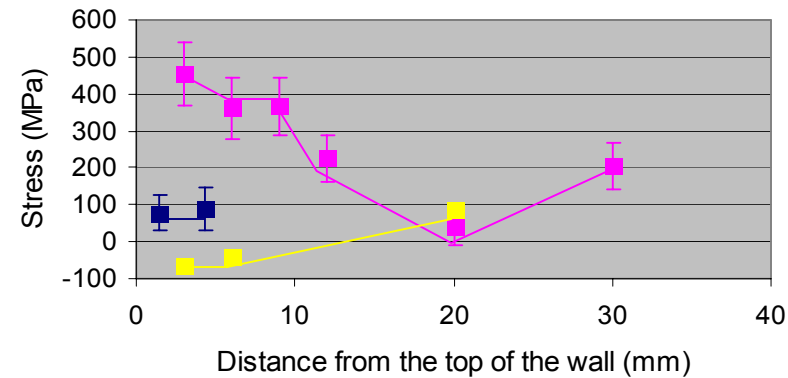
➤ After bench test with breaking

- Instrument: Neutron Diffractometer E3, HMI of Berlin (D)
- Wavelength: 0.178 nm
- Gauge Volume: 2x2x2 mm³
- Diffracting plans: (311) for Al, (200) for SiC

Component geometry and measurement region

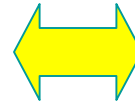
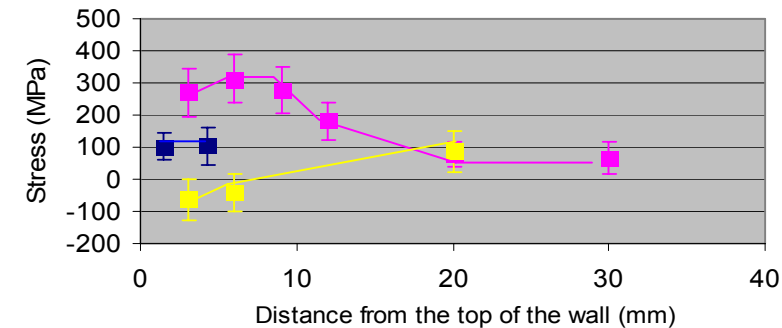


**Macrostress
Radial Direction**



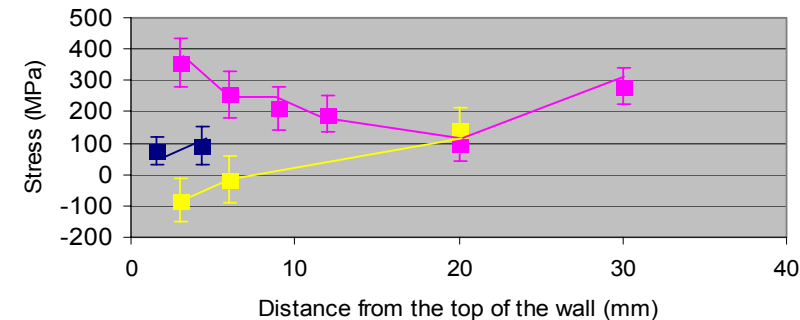
Residual macrostresses increase after the set of fatigue cycles without breaking.

**Macrostress
Axial Direction**



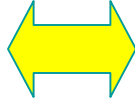
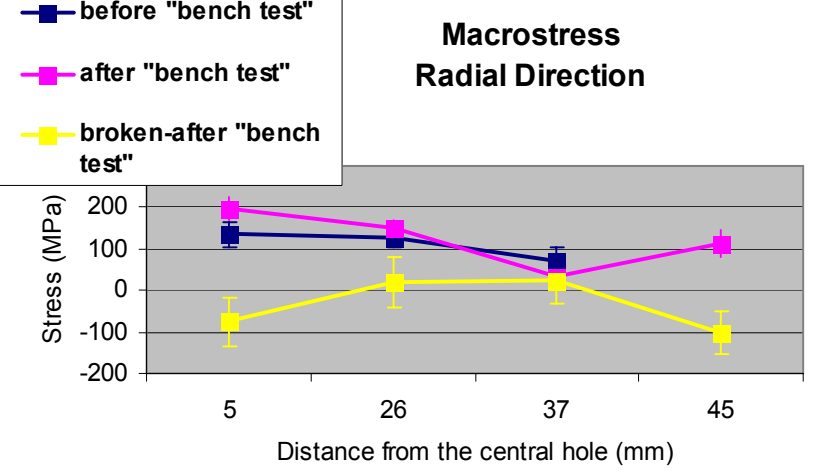
Hoop and radial directions correspond to the highest values of stress during the in-service life of the component.

**Macrostress
Hoop Direction**

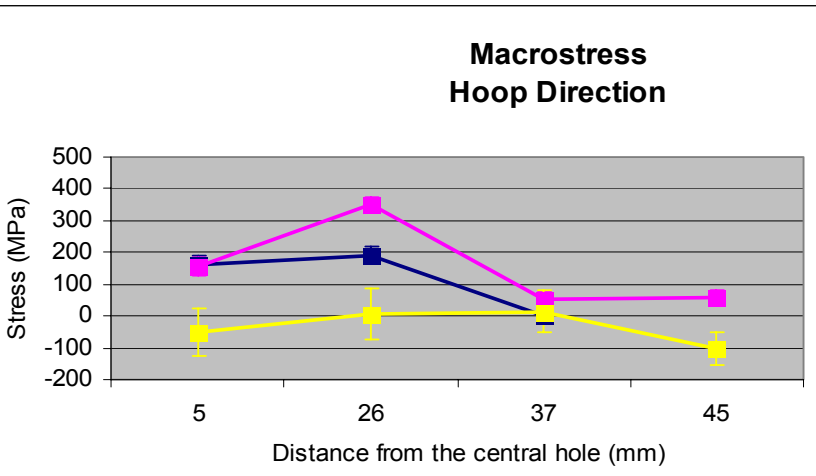
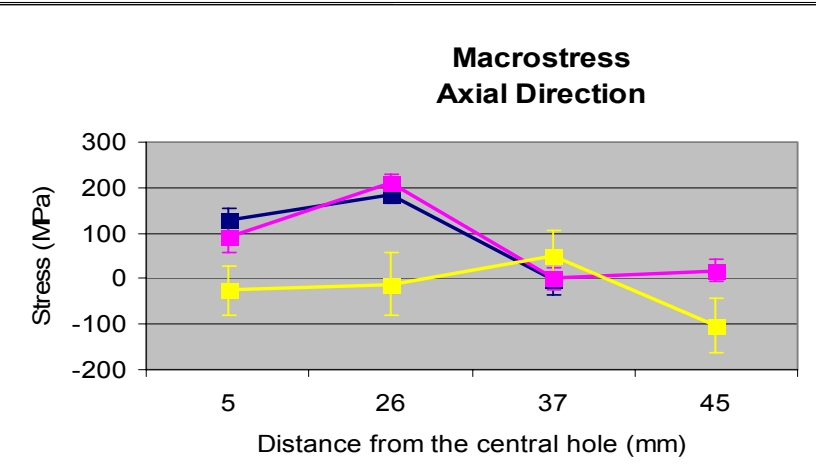


Macrostresses found before and after fatigue cycles add to the applied loads contributing to anticipate the component failure.

Macrostress



BOTTOM POINTS



Wheel Hub (AA6061 + 22 vol. % Al₂O_{3p})

3 identical wheel hubs → forging

T6: 560°C x 2 hours – H₂O at Room Temperature (RT) – 177°C x 10 hours.

T6-special: 560°C x 2 hours – H₂O at 60°C – 177°C x 8 hours.

Forging temperature	Pressure ratio	Die temperature	Oven temperature
460°C ± 20°C	Piston speed 10 mm / sec	Upper: ~ 200°C Lower: ~ 200°C	500°C x 1h 30' max

1) As-forged

2) Forged + T6 heat treatment

3) Forged + special T6 heat treatment



➤ As-forged

- Instrument: Neutron Diffractometer G5.2, LLB of Saclay (F)
- Wavelength: 0.316 nm
- Gauge Volume: 2x2x2 mm³
- Diffracting plans: (200) for Al, (113) for Al₂O₃

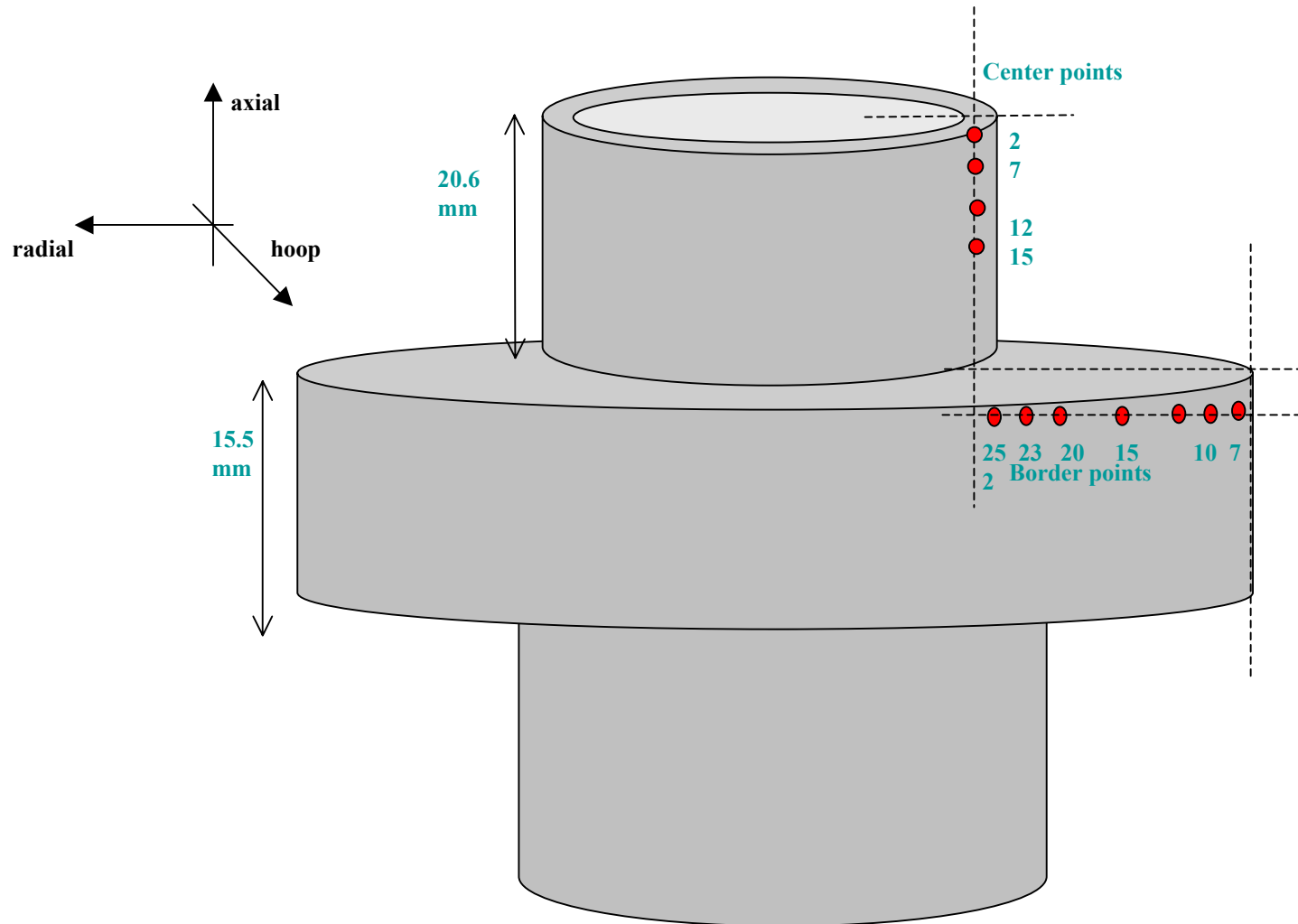
Forged + T6

- Instrument: Neutron Diffractometer D1A, ILL of Grenoble (F)
- Wavelength: 0.299 nm
- Gauge Volume: 2x2x2 mm³
- Diffracting plans: (311) for Al, (113) for Al₂O₃

➤ Forged + T6-special

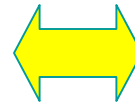
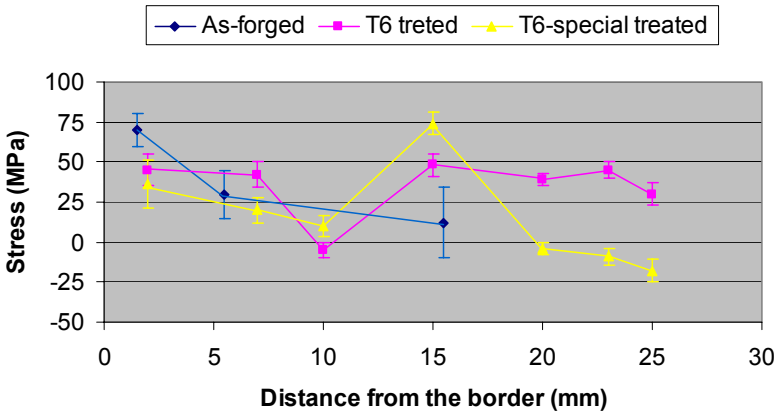
- Instrument: Neutron Diffractometer D1A, ILL of Grenoble (F)
- Wavelength: 0.299 nm
- Gauge Volume: 2x2x2 mm³
- Diffracting plans: (311) for Al, (113) for Al₂O₃

Wheel hub - Measurement points

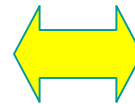


Macrostress

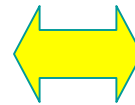
Radial Macrostress



Before heat treatments, the macrostresses are mainly located close to the border (in radial and hoop directions).



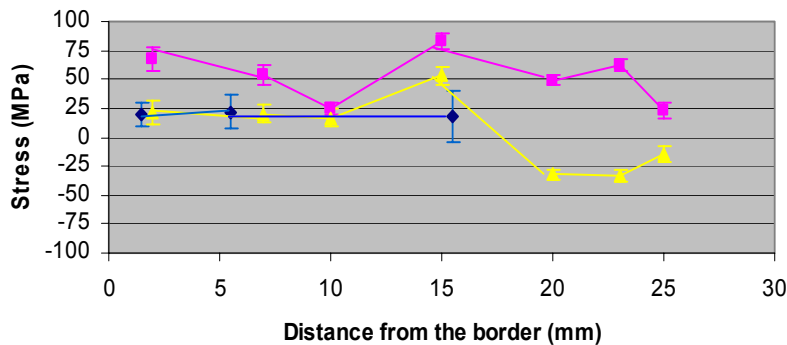
Radial and hoop macrostress at the surface are reduced by T6 heat treatment.



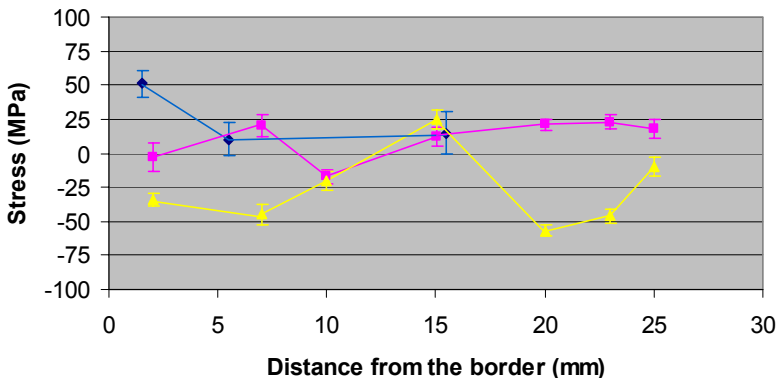
In the case of the T6-special treated hub, the macrostresses are lower than in the previous case (T6 treatment).



Axial Macrostress



Hoop Macrostress



T6 and T6-special treatments improve mechanical performances, because they reduced residual macrostress close to the surface, in the directions (hoop and radial) critical during service.

$$\sigma_{\text{tot}}^i = \sigma_{\text{macro}} + \sigma_{\text{mE}}^i + \sigma_{\text{mT}}^i$$

i = Matrix, Reinforcement

Difference in
elastic constants of
the two phases

Difference in
thermal expansion
coefficients of the
two phases

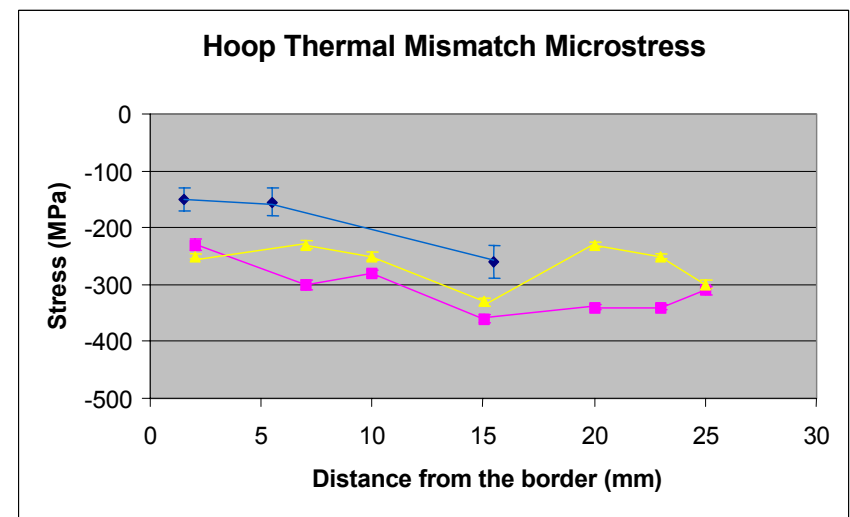
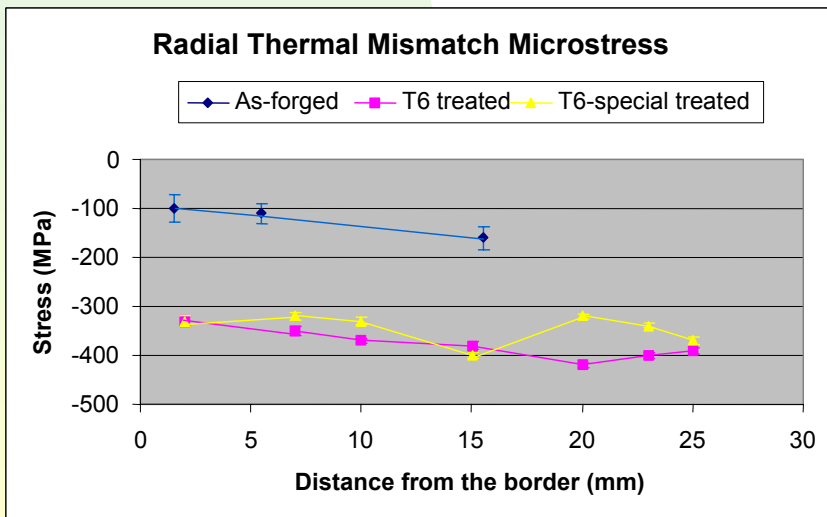
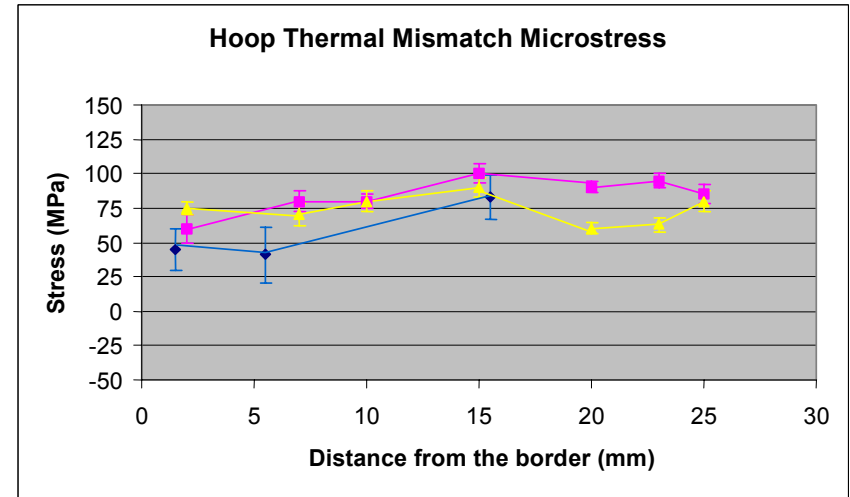
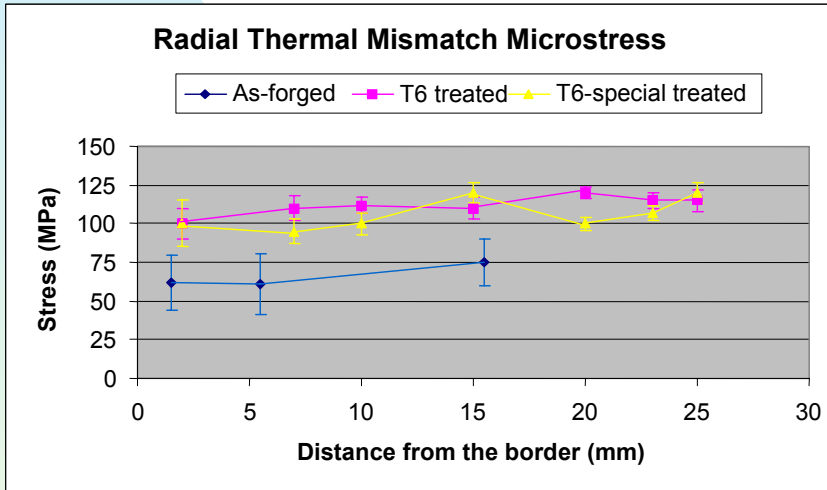
Negligible

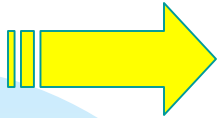
microstress monitoring

after mechanical and/or thermal treatments

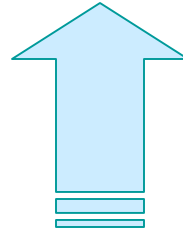
Thermal mismatch Microstress

WHEEL HUB (BORDER POINTS)



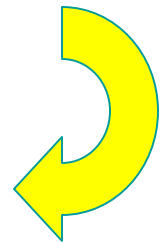


Thermal mismatch microstresses increase (in absolute value) after T6 and T6-special heat treatments.



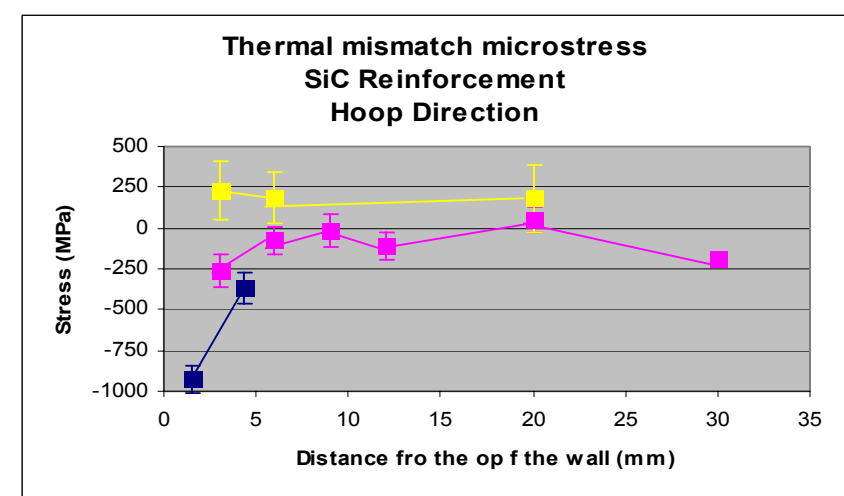
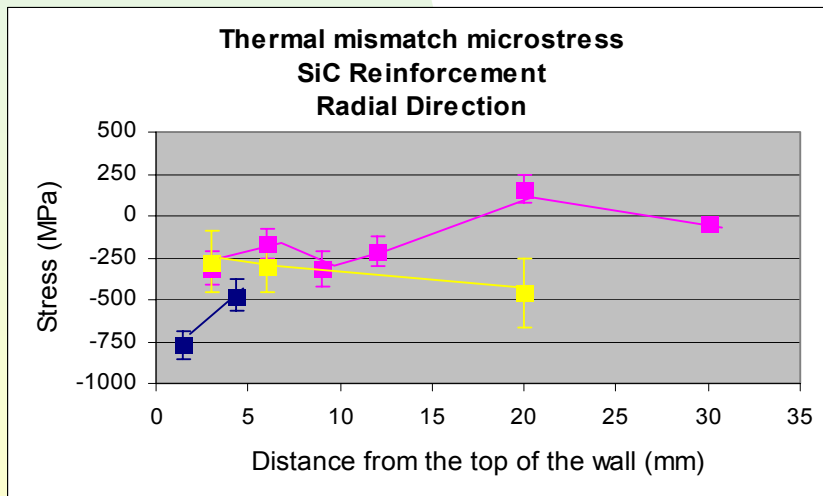
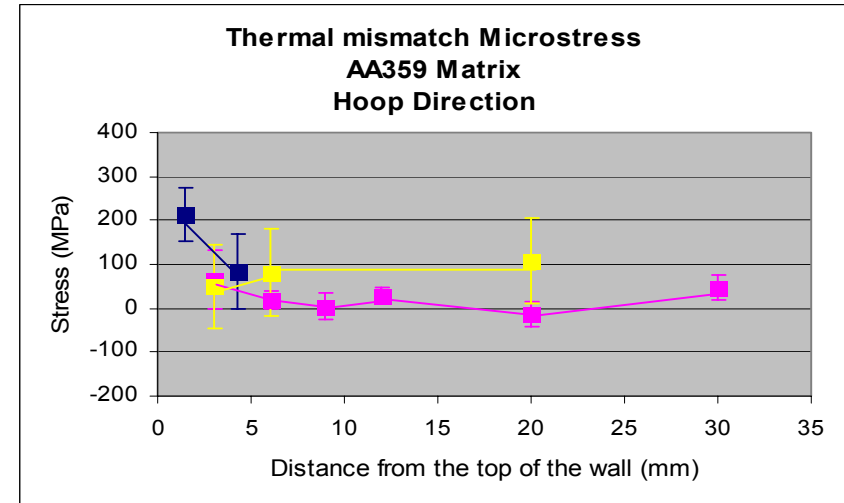
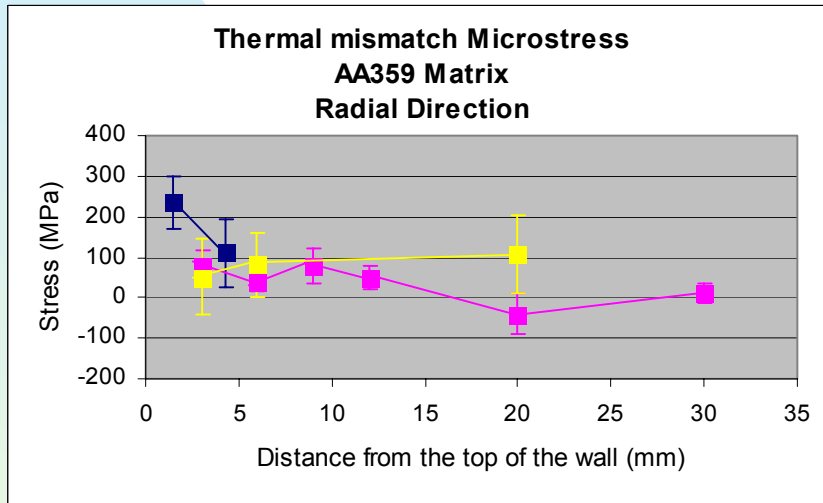
Reduced effect in the T6-special treated hub

T6-special treatment:



Good compromise to reduce macrostress without having too high thermal mismatch microstresses values.

Fatigue cycles induce a thermal microstress releasing



Conclusions

AA359+SiC Brake Drum

AA6061+Al2O3 Wheel Hub

RESIDUAL MACROSTRESS



AFTER FATIGUE CYCLES



AFTER T6 AND T6-SPECIAL TREATMENTS (SURFACE)

THERMAL MISMATCH MICROSTRESS

**RELEASE AFTER FATIGUE CYCLES
IN BOTH THE PHASES**

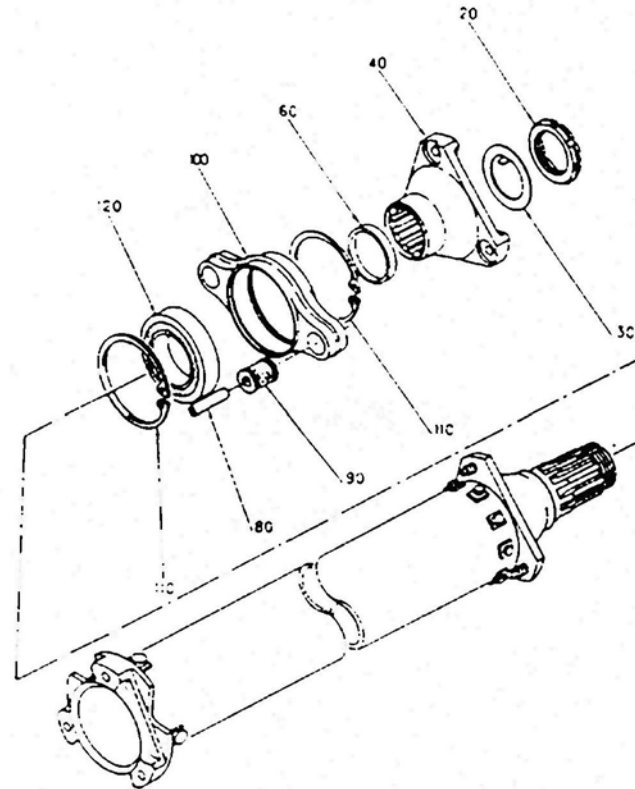
**INCREASE AFTER T6 AND T6-SPECIAL
TREATMENTS IN BOTH THE PHASES**

*Simulation of the forming process and comparison between
calculated and experimental results*

The present study is part of the European project COFCOM
(contract N° BRPT-CT97-803).

HMI-BENSC is acknowledge for beamtime allocation and
financial support in the frame of the EU programme “Access to
Large Scale Facilities”.

Component: Drive Shaft for Helicopter



Material: MMC AA2009 + 25% SiCp

Matrix composition:

	Cu	Mg	Si	O	Fe	Zn	other	Al
Min	3,2	1	-	-	-	-	-	remaining
Max	4,4	1,6	0,25	0,60	0,20	0,10	0,15	

Reinforcement:
SiCp particles

H and Cubic structure

The complete study has been carried out in several steps:

- 1/ Characterisation of the billet as fabricated (Powder Metallurgy)
- 2/ Characterisation of the test specimens after tensile tests
- 3/ Results used as input for the model to simulate the extrusion process
- 4/ Extrusion of a thick tube with the conditions simulated
- 3/ Characterisation of the demonstrator (thick tube $\text{\O}80\text{mm}$ thickness 19 mm as extruded and after T4 thermal treatment (498°C for 4h, followed by water quenching and natural ageing)

We will present only the University of Ancona's work on the residual stress analysis (points 1 and 5) and compare these results with the numerical simulation performed by the University of Galway (Ireland) (point 3).

The characterisation of the tensile specimen has been performed by the University of Catalunya (Barcelona, Spain), and the extrusion by British Aluminium (Redditch, Great Britain)

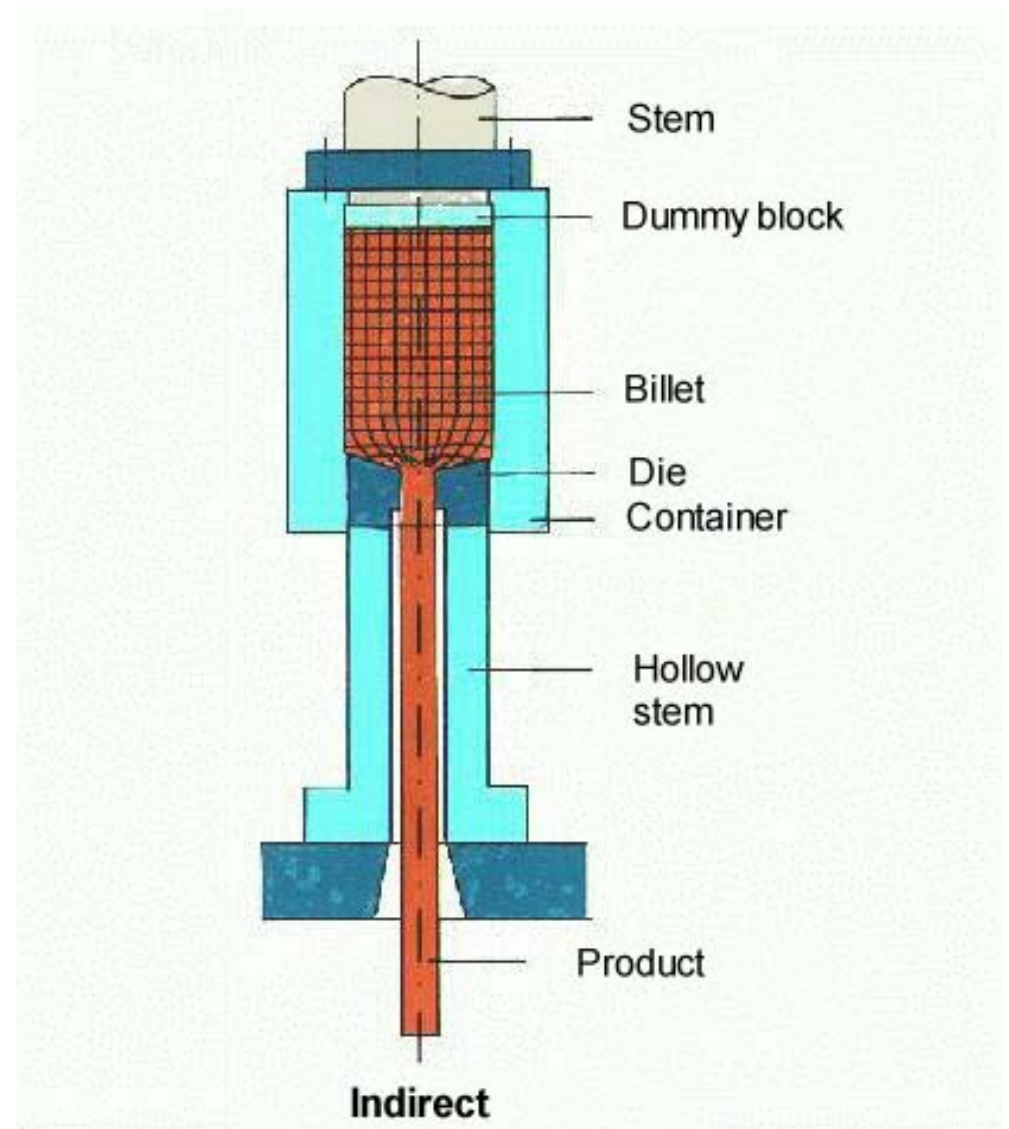
Extrusion process: indirect extrusion

Parameters:

θ container: 430°C

θ billet: 465°C

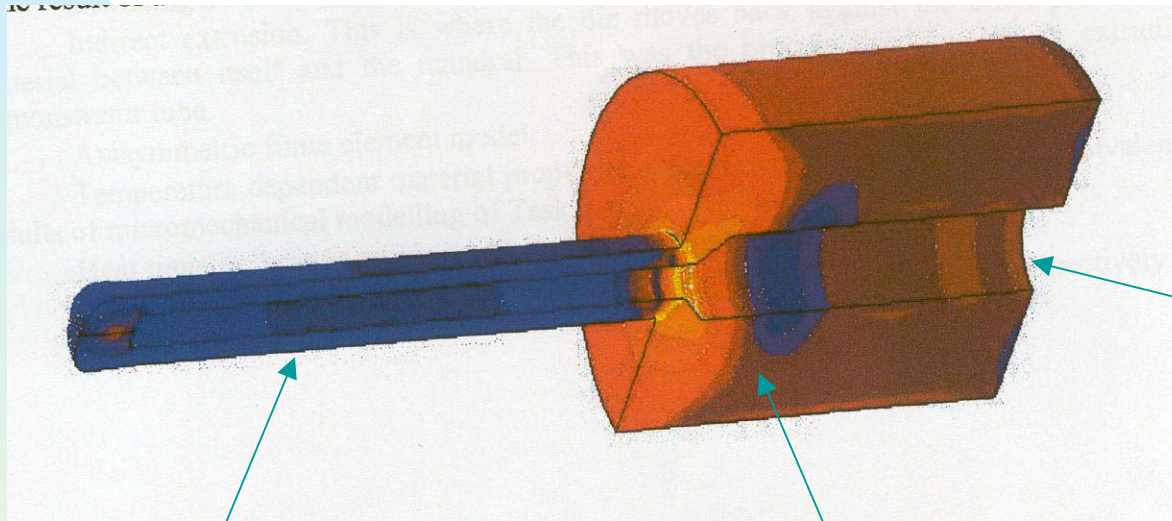
Speed: 0,5m/mn



• **Billet** prepared by standard powder metallurgical route (as fabricated) with dimensions 356 mm diameter, 30 mm height.

Very low residual stresses: around 10 MPa in the aluminium and -50 MPa in the SiC.

Simulation of the extrusion process



Direction of extrusion

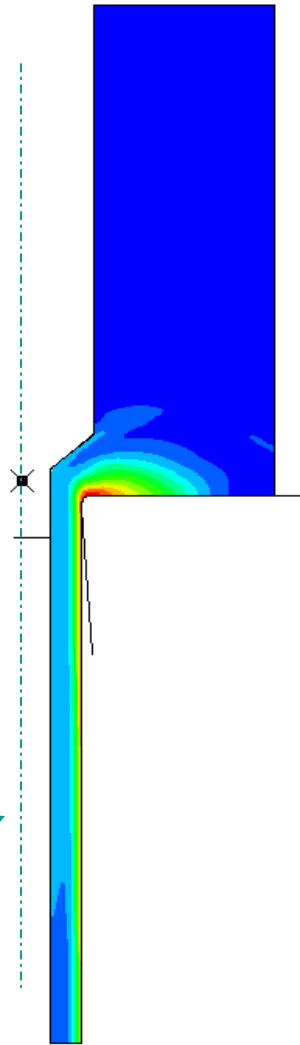
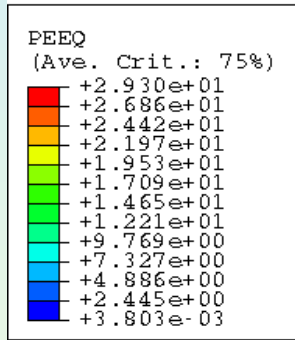


Extruded tube

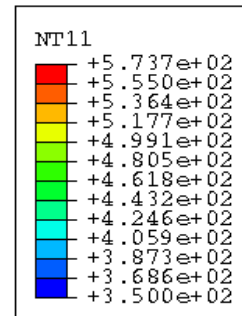


Results of the simulation

(a)



(b)



Mandrel

Billet

Tube

Axis of the cylindrical symmetry

Distribution of (a) equivalent plastic strain and (b) temperature ($^{\circ}\text{C}$).

The temperature distribution and the equivalent plastic strain at the end of the extrusion process are essentially constant in depth and along the cylinder axis.

The temperature gradient through the extruded tube is insignificant \Rightarrow the residual stress in the tube will not be affected by uniform cooling.

Experimental results

	Macro Stress (MPa)			Average error ± 40 MPa
Sample	Axial	Radial	Hoop	
As extruded	74	69	71	
T4	80	27	43	

Table 1: Macro

T4 thermal treatment



the *macro-stress* relaxes in the radial and hoop directions and remains constant in the axial one

	Al Average error: ± 35 MPa			SiC Average error: ± 35 MPa		
Sample	σ_{ax}	σ_{rad}	σ_{hoop}	σ_{ax}	σ_{rad}	σ_{hoop}
As extruded	135	109	120	-109	-49	-73
T4	163	98	126	-171	-183	-206

Table 2: Total stress in the principal directions for the two tubes

T4 thermal treatment



Nevertheless, *total stresses* remain almost constant in the Al matrix and increase in the SiC reinforcement

	Al			SiC		
	Average error: ± 35 MPa			Average error: ± 35 MPa		
Sample	σ_{ax}	σ_{rad}	σ_{hoop}	σ_{ax}	σ_{rad}	σ_{hoop}
As extruded	83	40	49	-183	-118	-144
T4	83	71	83	-251	-210	-249

Table 3: Microstress in the principal directions for the two tubes

T4 thermal treatment



This implies that both the tensile *micro-stresses* in the Al phase and the compressive *micro-stresses* in the SiC phase increase (of about 30 MPa for the Al phase and 70 to 100 MPa for the SiC phase).

Although error bars are relatively large, this behaviour is to be expected and exceeds the confidence limits.

Conclusion

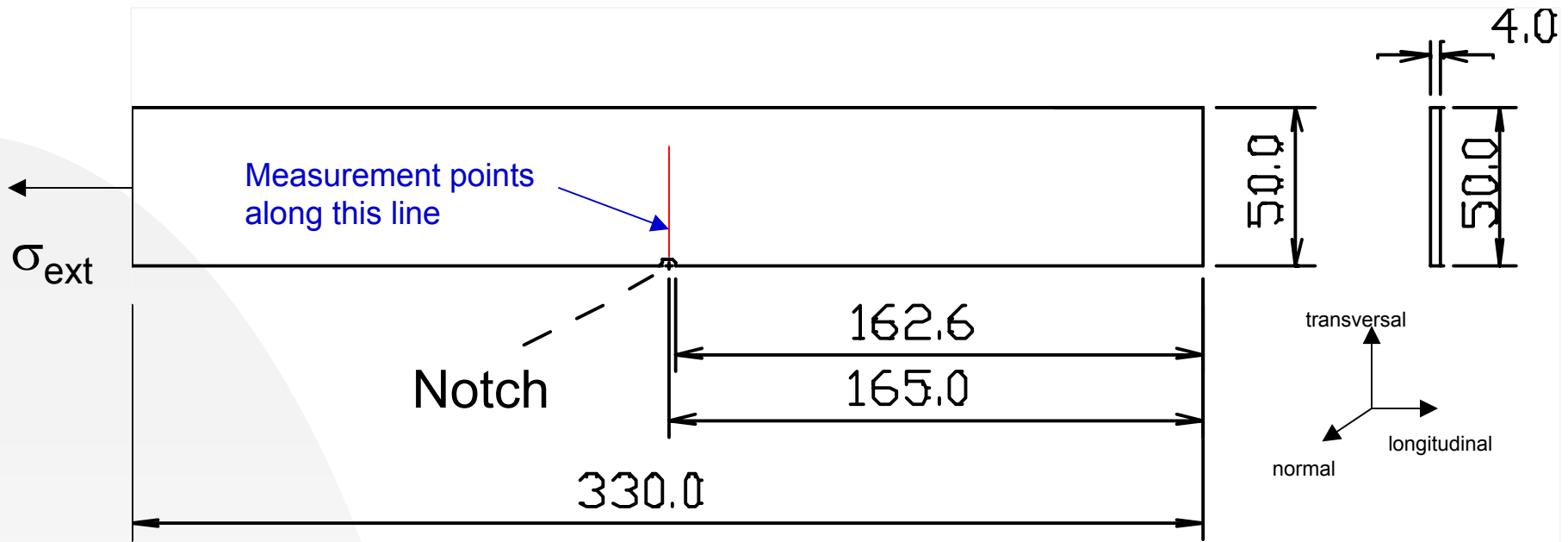
As expected, results show that the main contribution to residual stress is generally given by thermal microstresses.

If the macrostress is vanishing (in the billet) \Rightarrow thermal mismatch stresses stay very small

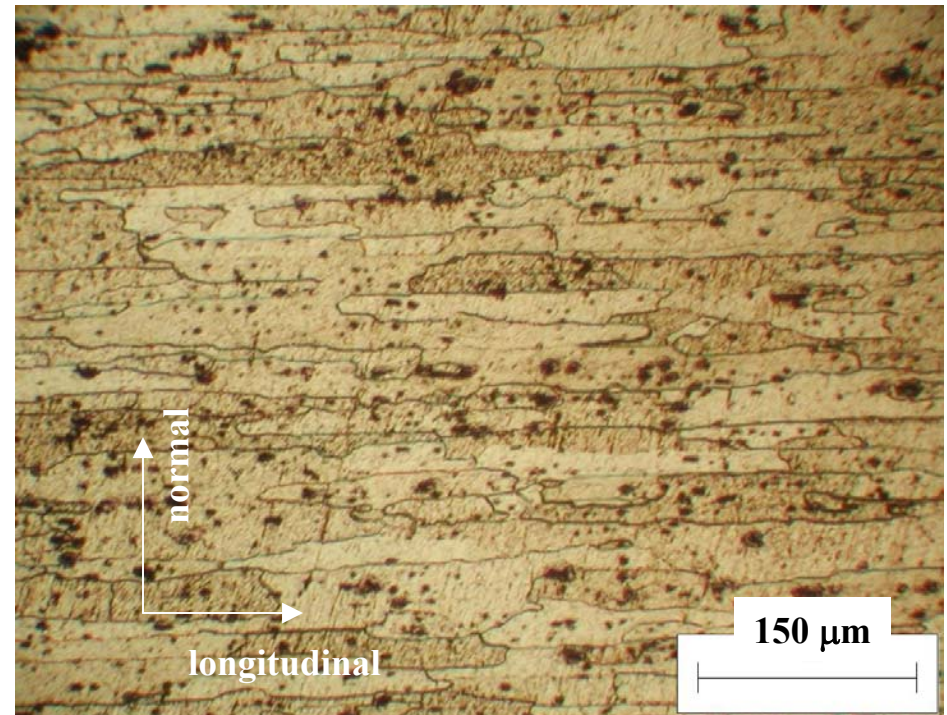
In the tube: macrostresses are constant along the thickness and decrease on application of the thermal treatment, while microstresses increase.

This effect can be observed only using Neutron Diffraction as evaluation technique.

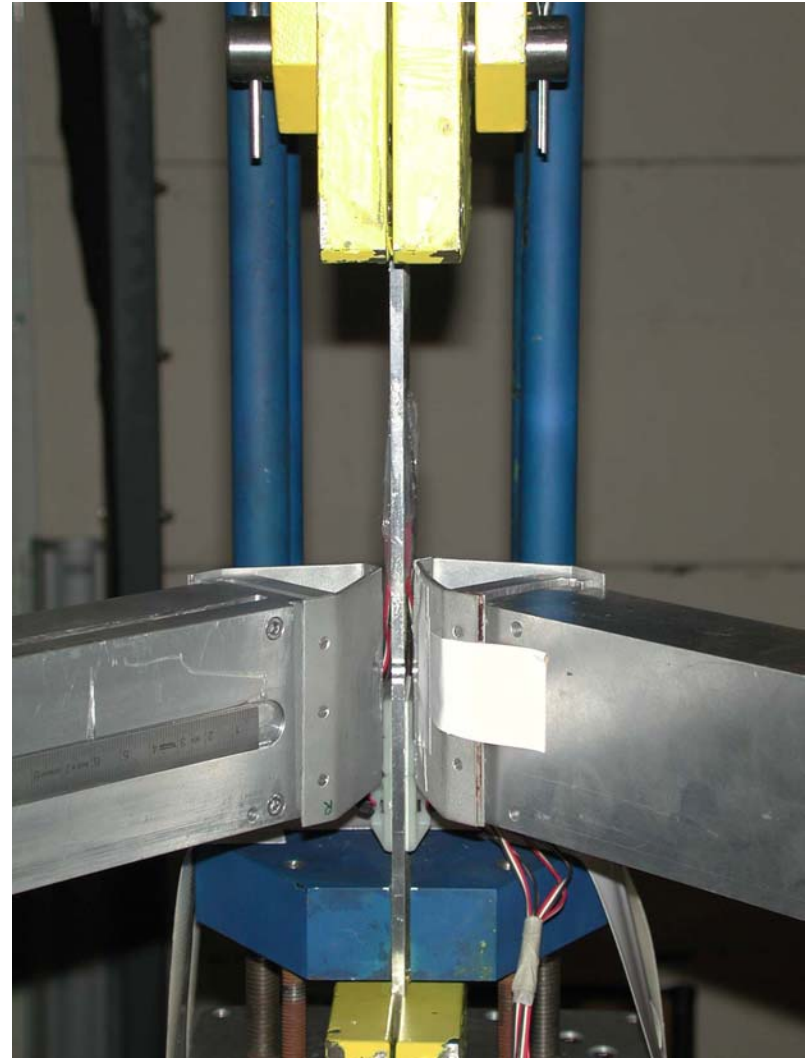
Numerical simulations are in good agreement with experiments and predict very low macrostress in the extruded tube.



- precycled: $R = 0.06$, $\sigma_{\text{max}} = 90$ MPa;
- **crack length**: about **4 mm** from the notch (transversal direction);
- **plane stress** assumed ($\sigma_{\text{normal}} = 0$), due to specimen geometry.

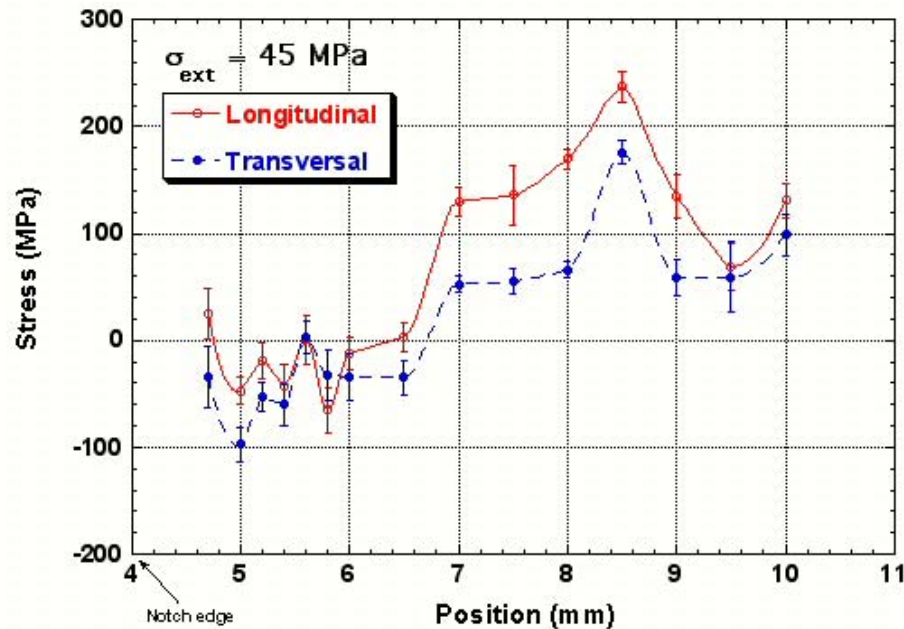
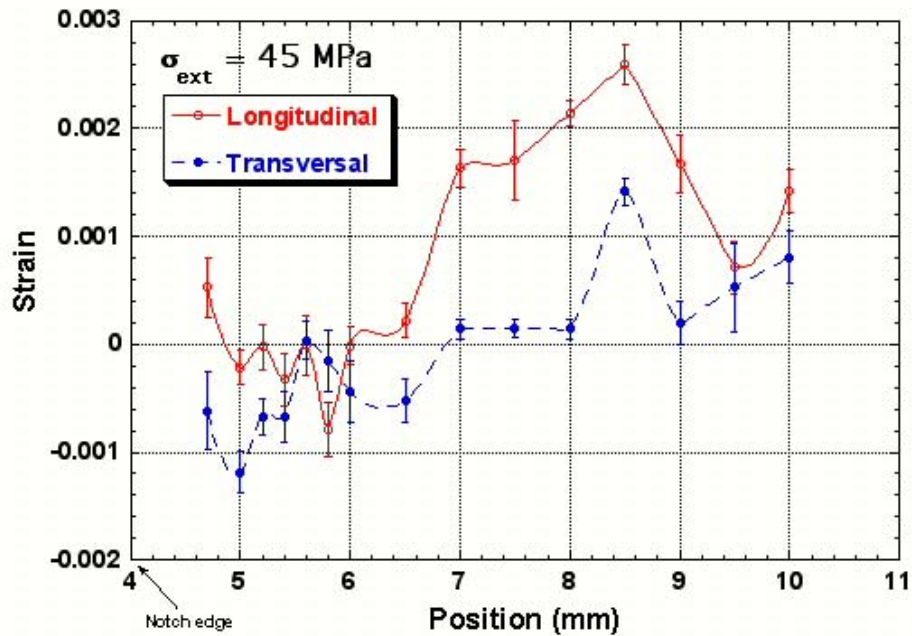


Measurements at LLB-Saclay



Experimental conditions

- $\sigma_{\text{ext}} = 45 \text{ MPa}$
- $\lambda = 0.33 \text{ nm}$, (111) Al Bragg peak
- gauge volume: $0.8 \times 0.5 \times 1 \text{ mm}^3$
- longitudinal and transversal strain directions investigated
- d_0 measured in a point far from the crack

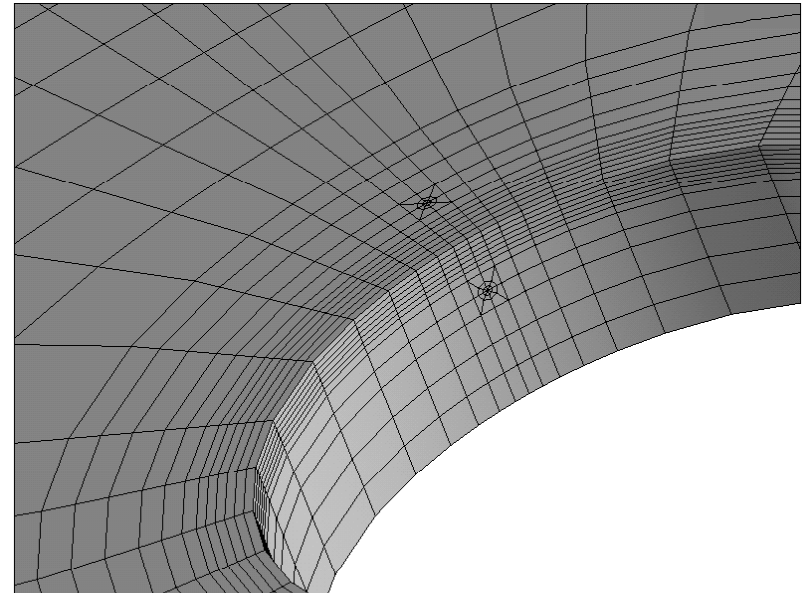
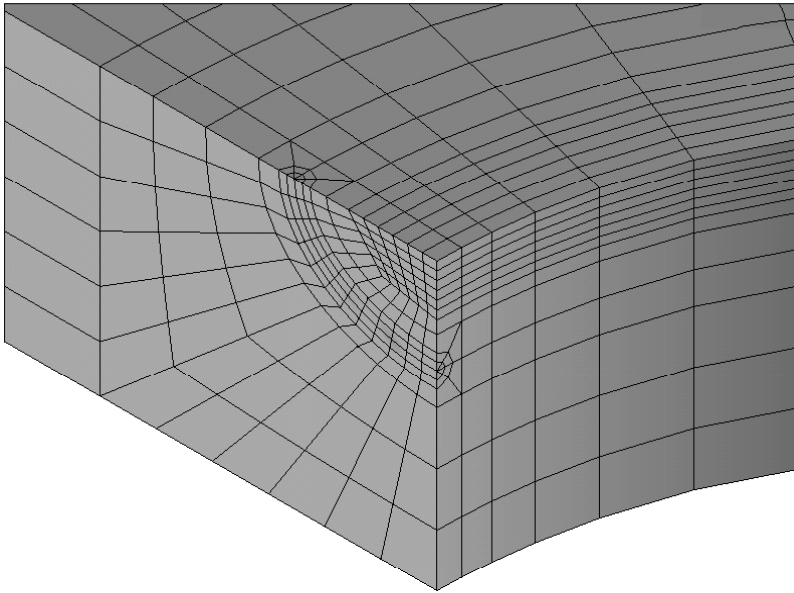


$$\sigma_L = \frac{E}{1 - \nu^2} (\varepsilon_L + \nu \varepsilon_T)$$

$$\sigma_T = \frac{E}{1 - \nu^2} (\varepsilon_T + \nu \varepsilon_L)$$

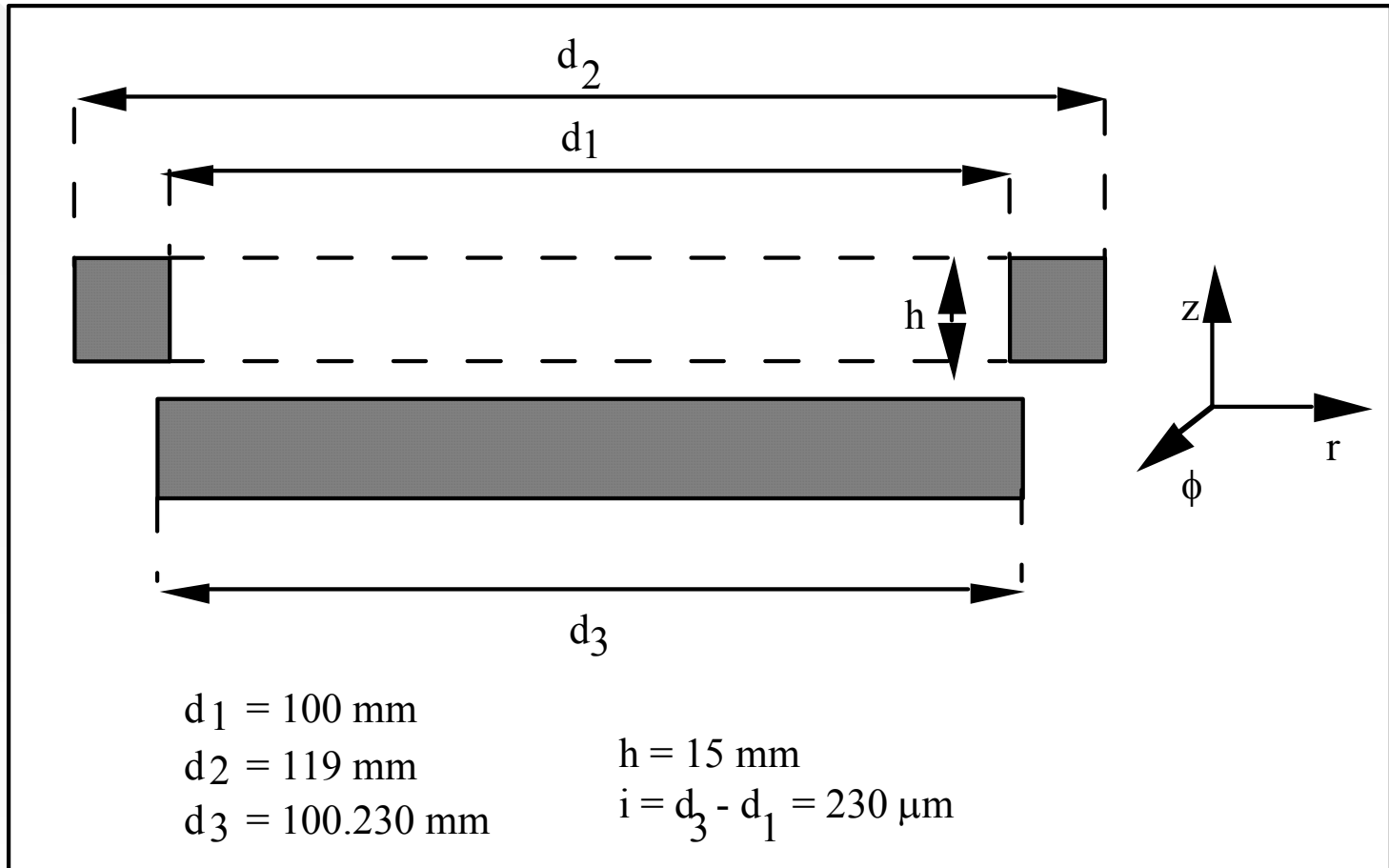
$$\sigma_N = 0$$

- Results will be compared with **FEM calculations** (carried out by University of Naples)



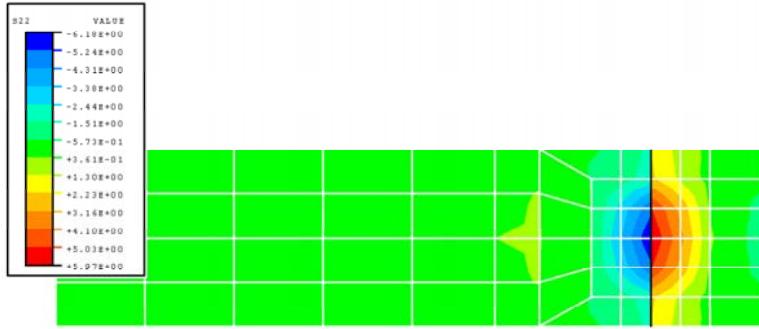
- **Short crack** (0.2 mm) recently investigated by **synchrotron radiation** (6-10 Nov. @ ESRF - data analysis in progress)

AA6082 Shrink-Fit Systems



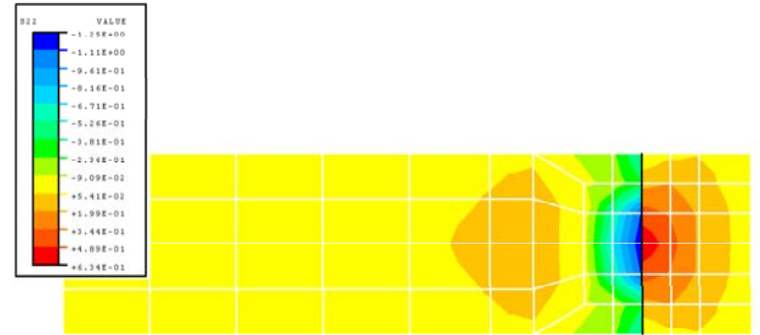
FEM RESULTS

Thermoelastic

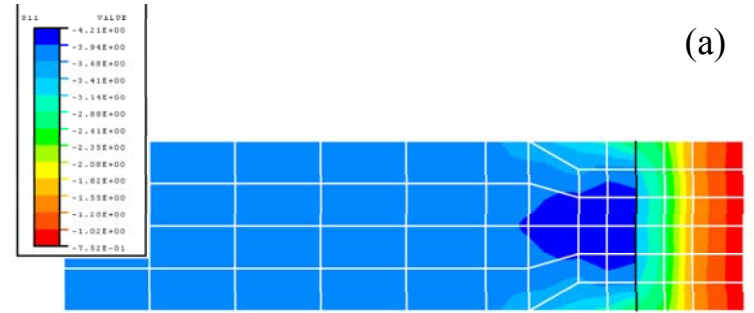


(a)

Thermoelastoplastic



(a)



(b)

(b)

(c)

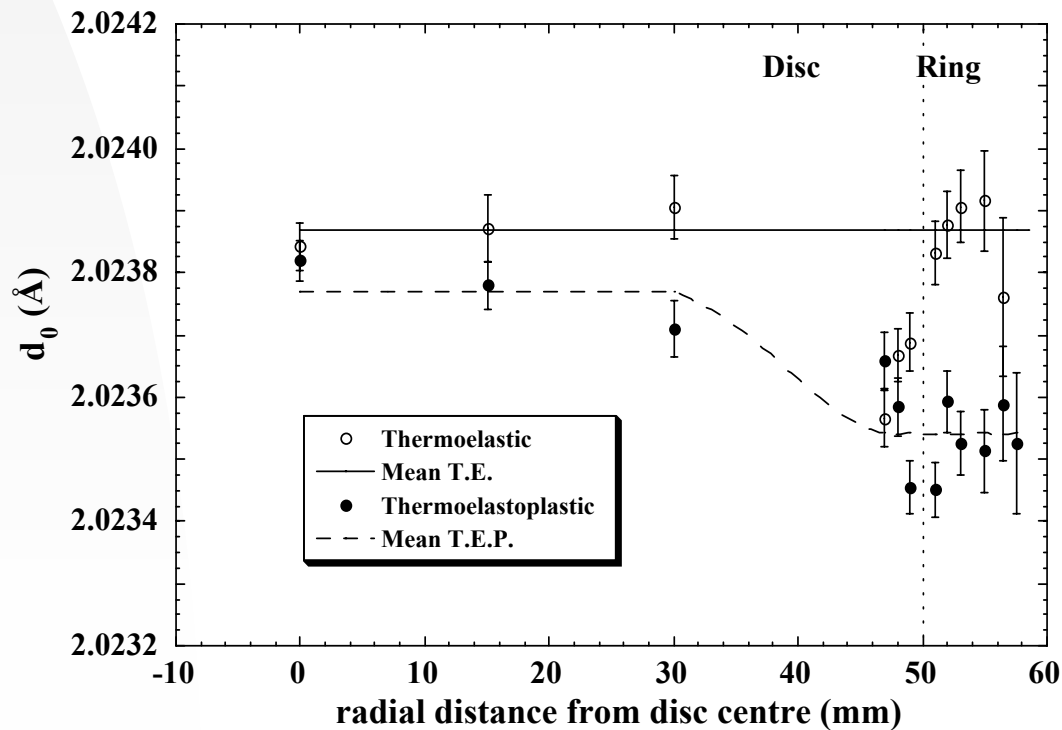
(c)

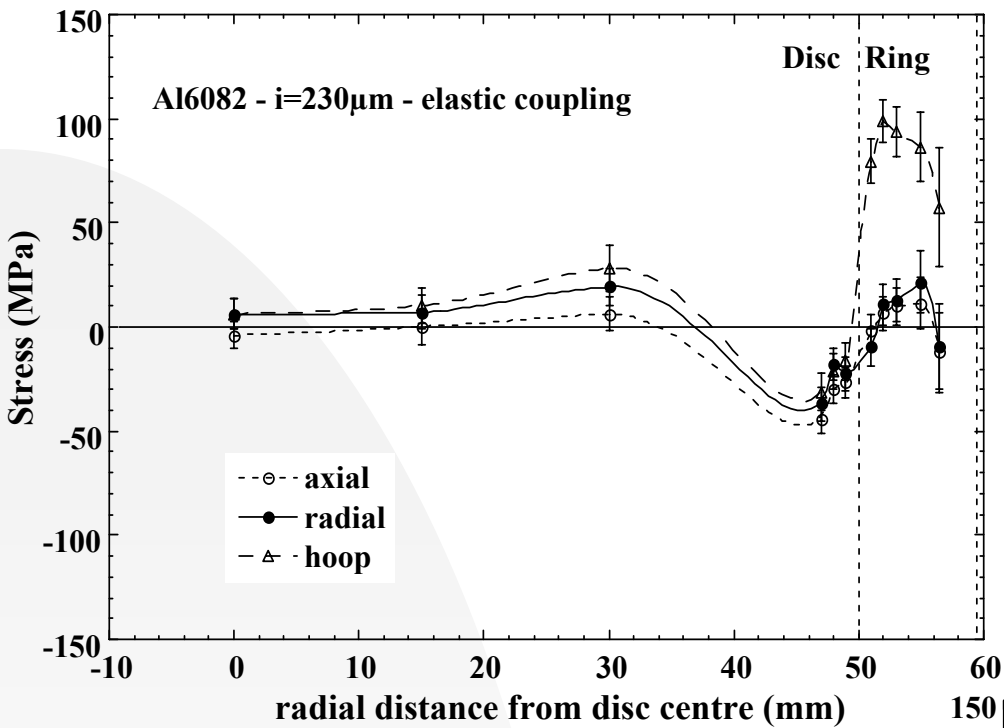
a) axial; b) radial; c) hoop

NEUTRON DIFFRACTION

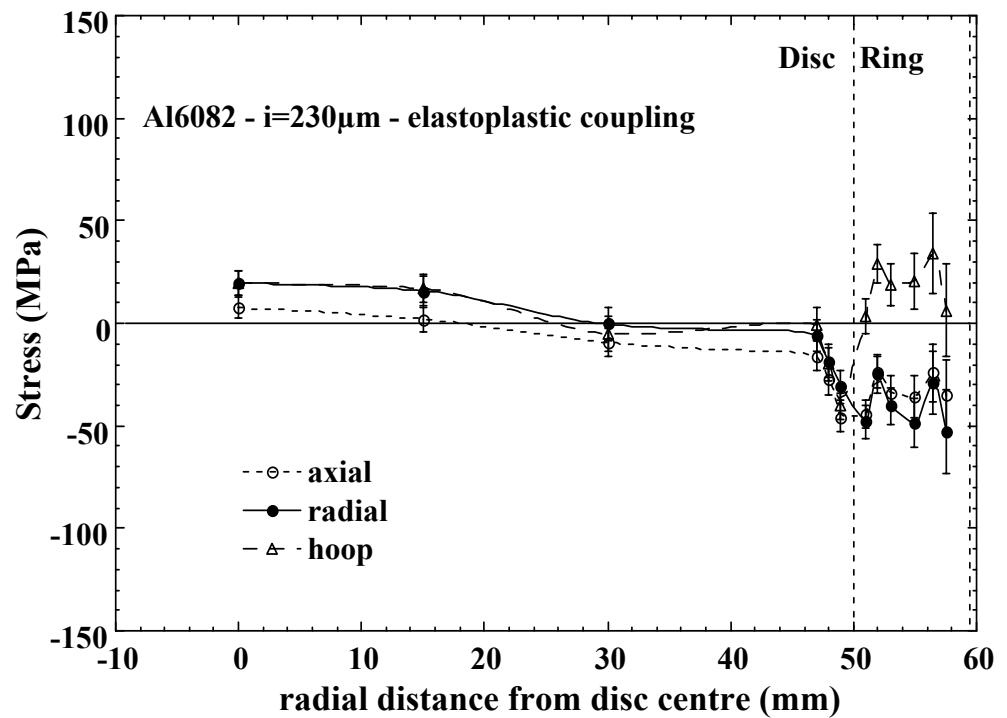
- G5.2 diffractometer of LLB, Saclay (F)
- (200) Bragg peak was used ($d_{200} \approx 2.024 \text{ \AA}$)
- neutron wavelength $\lambda = 2.84 \text{ \AA}$
- 13 gauge points were investigated (6 in the disc, 7 in the ring)
- gauge volume = 1.1 mm (basis diameter) x 3 mm (height) cylinder

Unstrained interplanar distance d_0 (imposing biaxial stress):

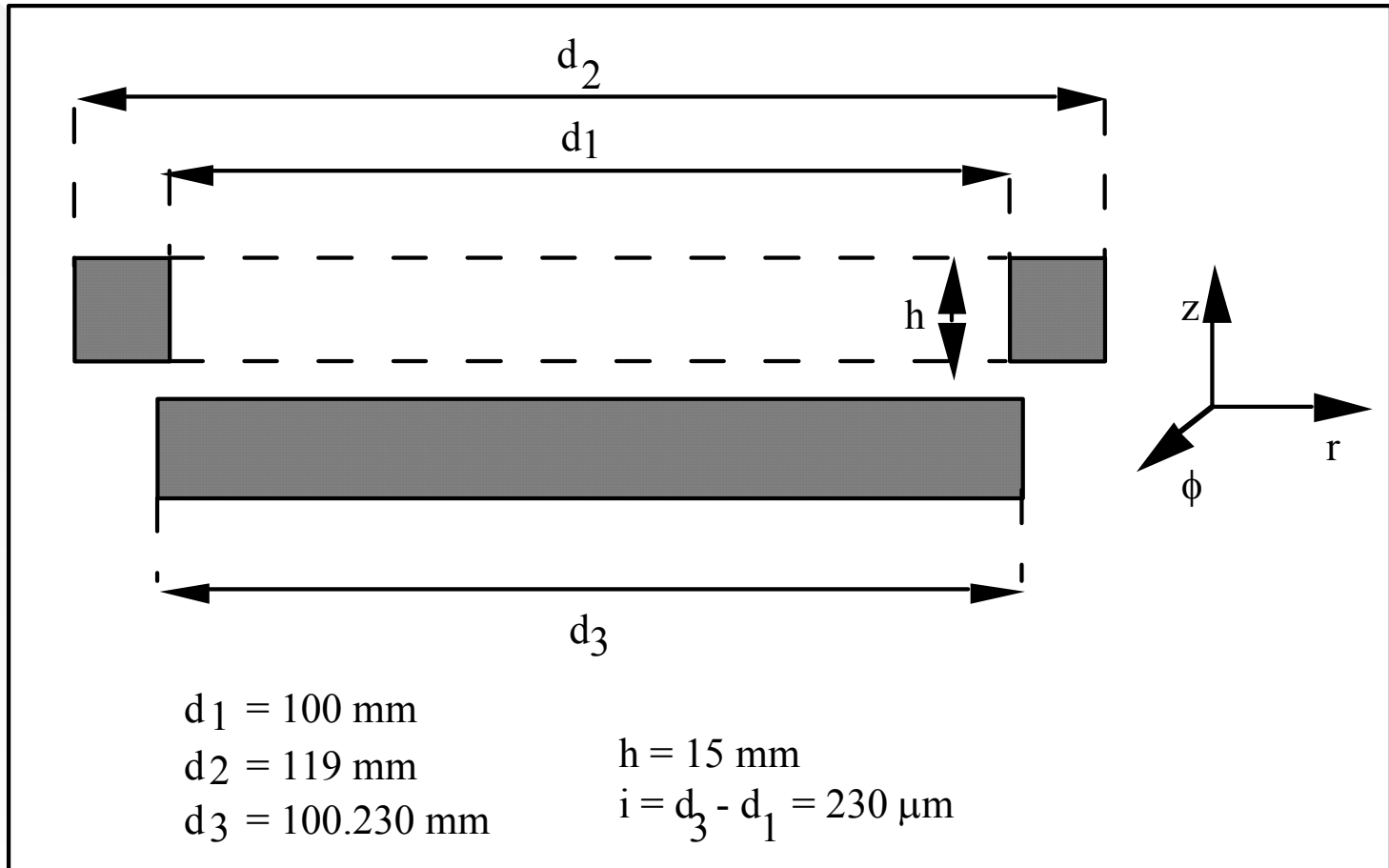




Good agreement with FEM calculations

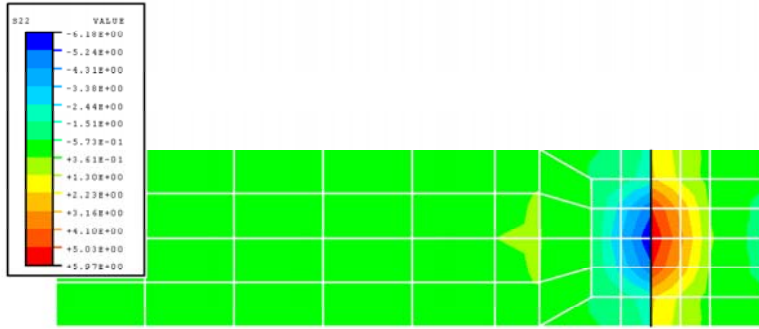


AA6082 Shrink-Fit Systems



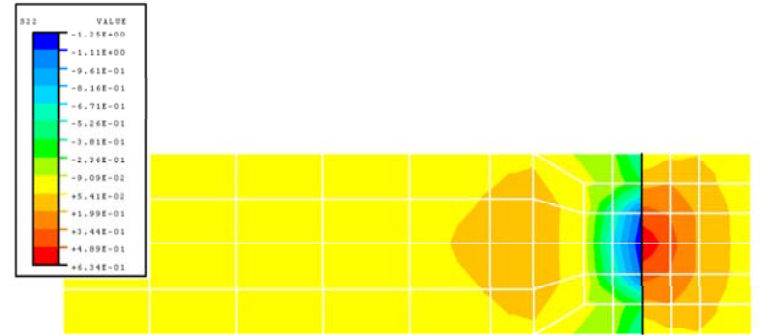
FEM RESULTS

Thermoelastic

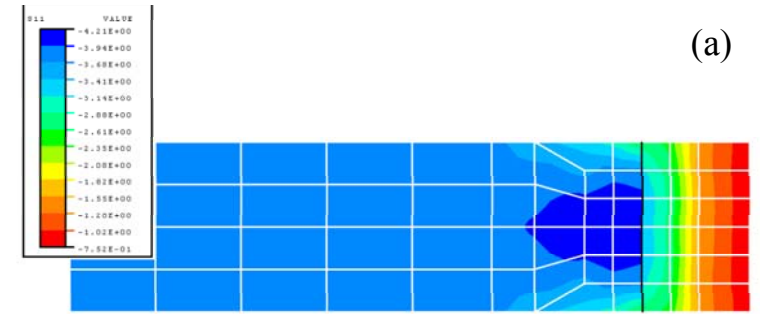


(a)

Thermoelastoplastic



(a)



(b)

(b)

(c)

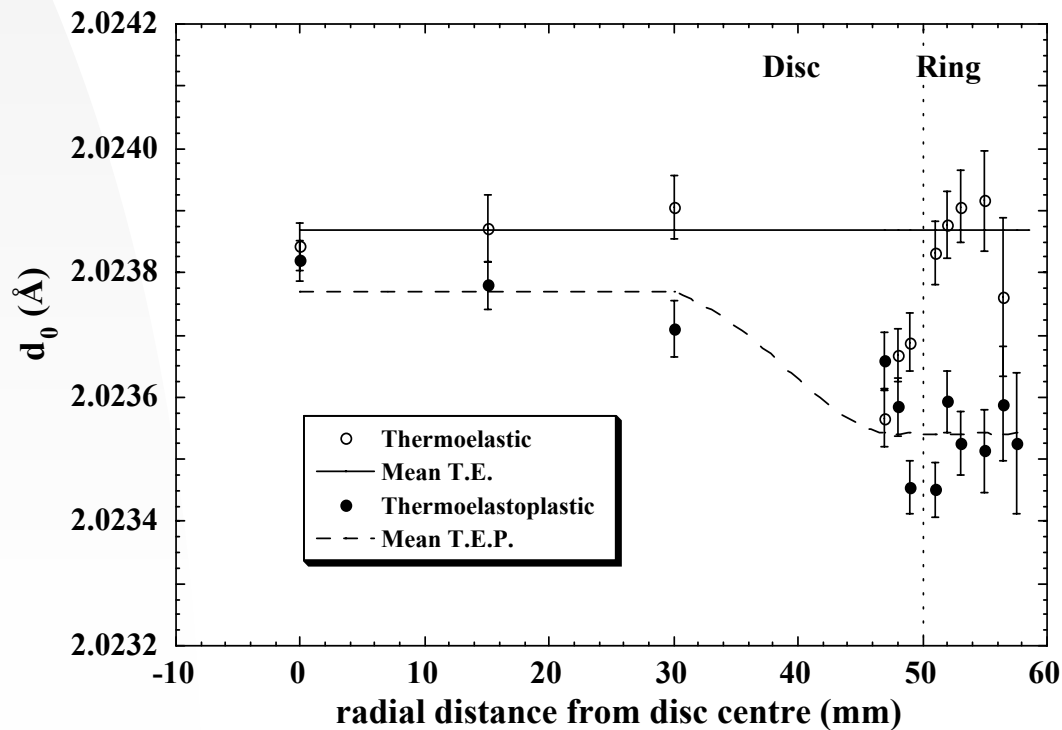
(c)

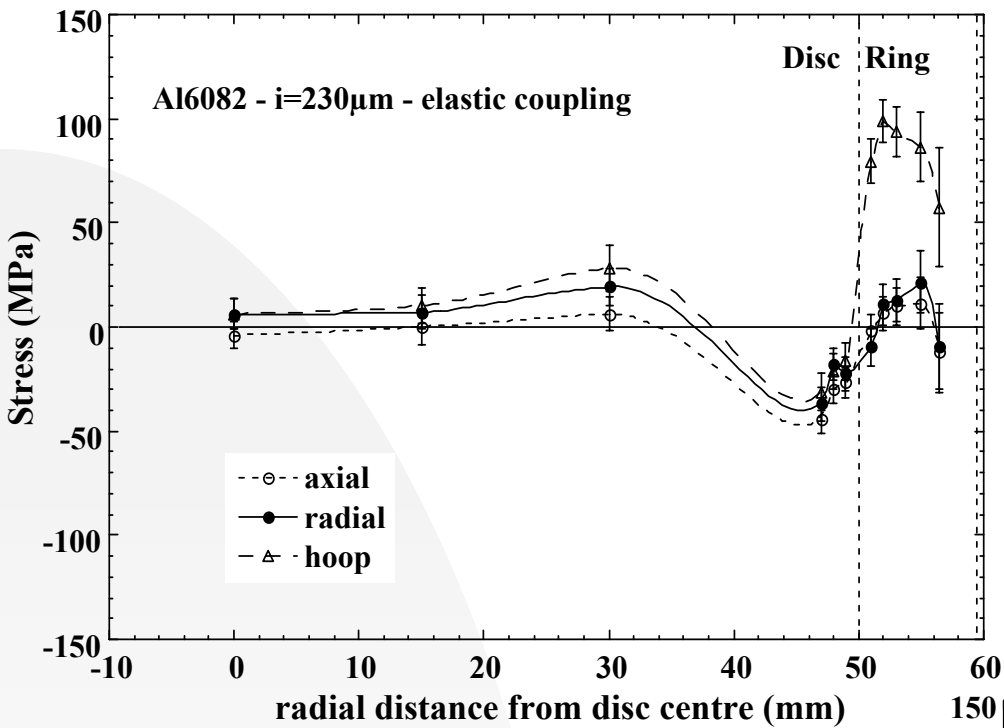
a) axial; b) radial; c) hoop

NEUTRON DIFFRACTION

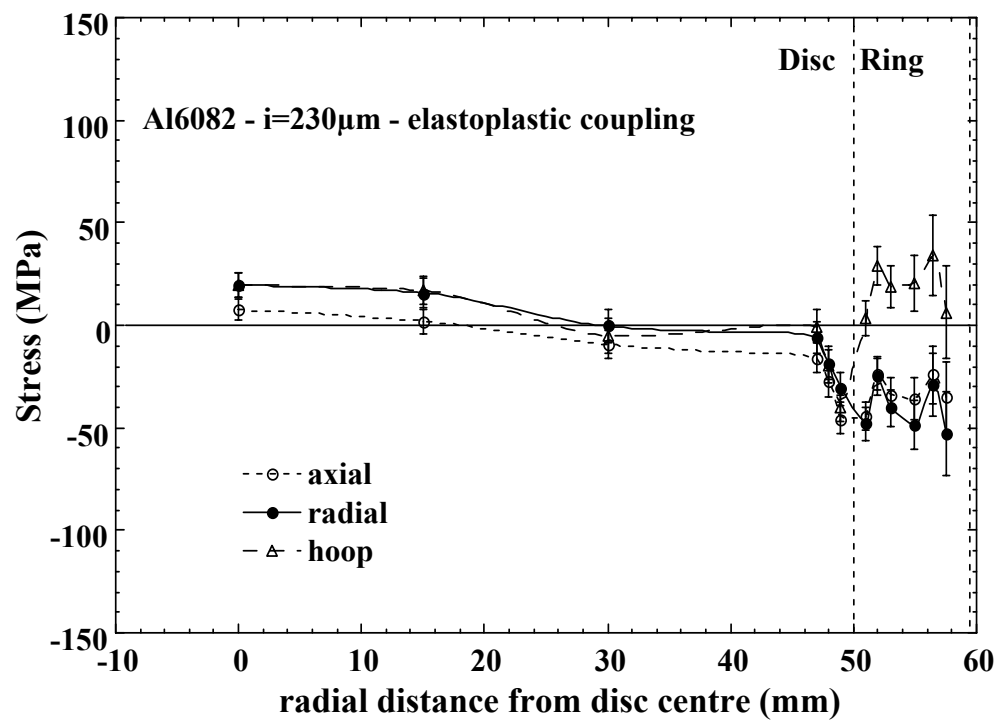
- G5.2 diffractometer of LLB, Saclay (F)
- (200) Bragg peak was used ($d_{200} \approx 2.024 \text{ \AA}$)
- neutron wavelength $\lambda = 2.84 \text{ \AA}$
- 13 gauge points were investigated (6 in the disc, 7 in the ring)
- gauge volume = 1.1 mm (basis diameter) x 3 mm (height) cylinder

Unstrained interplanar distance d_0 (imposing biaxial stress):

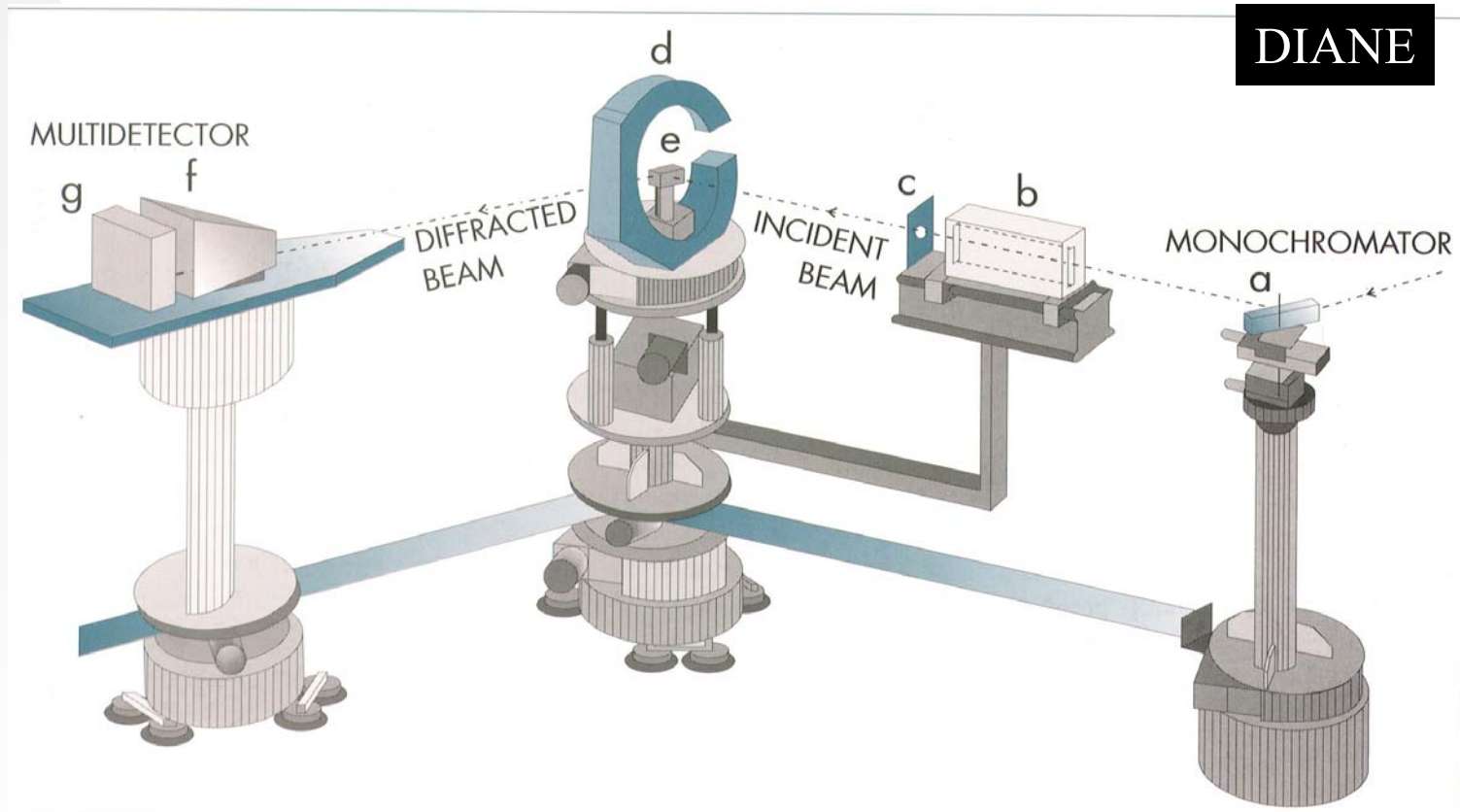




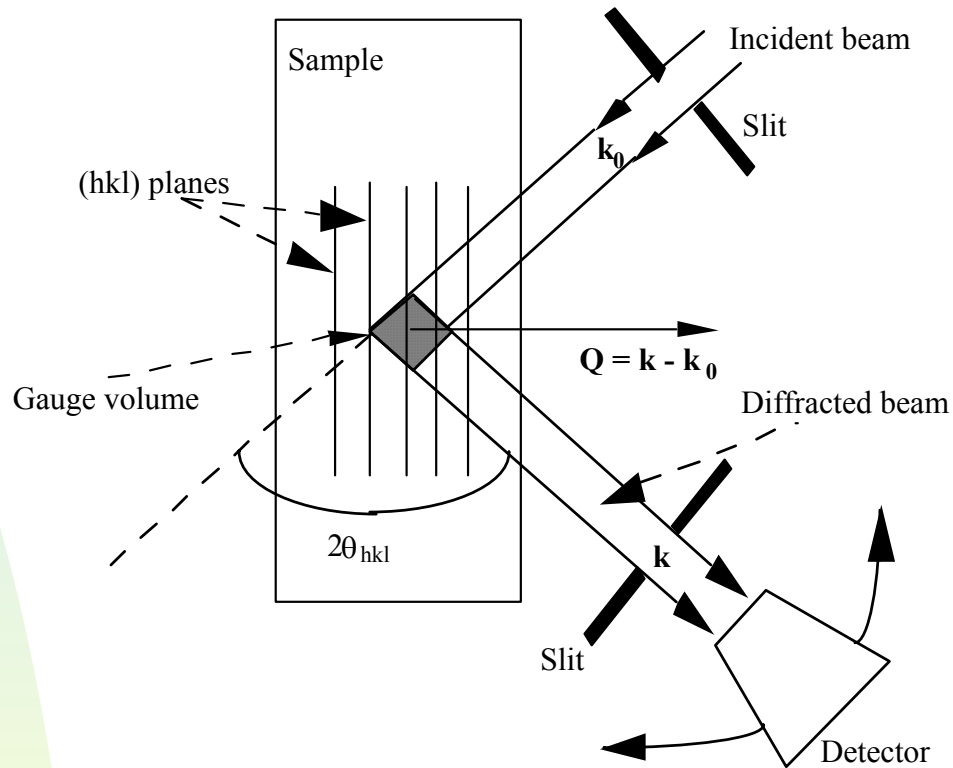
Good agreement with FEM calculations



Neutron diffraction for residual stress determination



Residual stress measurements by neutron diffraction

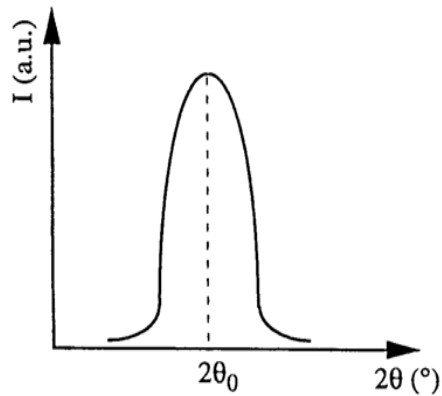


k_0 = wave vector of incident neutrons

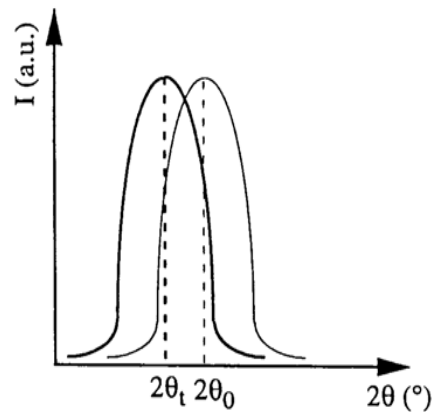
k = wave vector of diffracted neutrons ($|k| = |k_0|$)

$Q = k - k_0$ = scattering vector

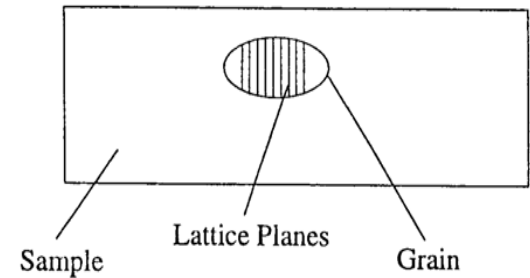
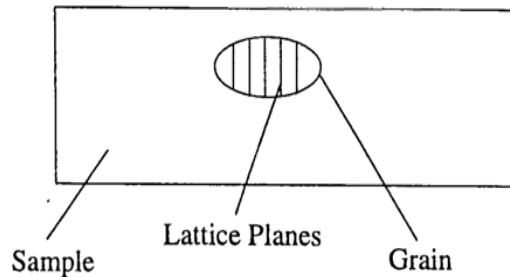
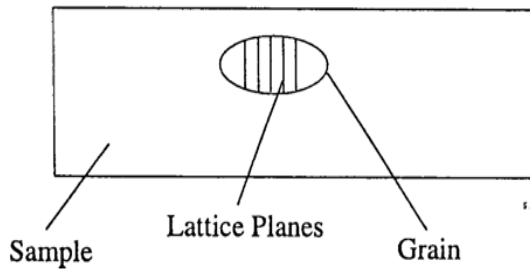
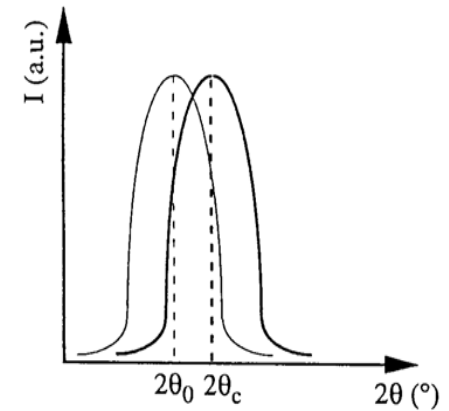
Unstrained sample



Tensile stress



Compressive stress



Bragg's Law: $\lambda = 2d_{hkl} \sin\theta_{hkl}$
(d_{hkl} = interplanar distance for hkl planes)

Strain: $\epsilon = (d_{hkl} - d_{0,hkl}) / d_{0,hkl}$
(d_0 = "unstrained" interplanar distance)

- **Choose the (hkl) planes** to be investigated and adjust the neutron wavelength so that the Bragg's law is fulfilled for a given θ (usually $2\theta \approx 90^\circ$ for the best definition of the gauge volume)
- **Determine the precise position of the Bragg peak** and then the interplanar distance d_{hkl} by the Bragg's law
- **Evaluate the strain as**

$$\varepsilon = \frac{d_{hkl} - d_{0hkl}}{d_{0hkl}}$$

where d_{0hkl} is the unstrained interplanar distance

- **Repeat the measurements in several spatial directions** to determine the six components of the strain tensor (only 3 directions if the principal strain axes are known)
- **Calculate stresses** by means of elasticity theory equations (Hooke's law)

Macro- and micro-stresses

- The macrostresses can be calculated from the measured stresses in both phases as follows:

$$\sigma_{macro} = f \sigma_{tot}^{Al_2O_3} + (1 - f) \sigma_{tot}^{Al}$$

where f is the volume fraction of the reinforcement.

- The microstresses (essentially thermal) in each phase are given by:

$$\sigma_{micro}^i = \sigma_{tot}^i - \sigma_{macro}$$

Follow-up of two European projects:

1) MISPOM “ Development of models for the prediction of the in-service performance of MMC components” (contract.n.BRPR-CT97- 0396)

2) COFCOM “Computer assisted optimisation of the forming process of MMC Components” (contract.n.BRPT-CT97- 803).

Partners: Aerospatiale (F), Centro Ricerche Fiat - Teksid (I), Defence Evaluation and Research Agency (UK), Erich Schmid Institut (AT), Stampal - Simbi division (I), British Aluminium Speciality Extrusions (UK), INFM - University of Ancona (I), Universitat Politecnica de Catalunya (ES), National University of Ireland (IE), Eurocopter (F).